BUNDESAMT FÜR
SEESCHIFFFAHRT
UND
HYDROGRAPHIE

WOCE
Global Hydrographic Climatology

A Technical Report

Autoren:
Gouretski, V. V.
Koltermann, K. P.

Berichte des
Bundesamtes für Seeschifffahrt und Hydrographie
Nr. 35/2004

In der Reihe „Berichte des Bundesamtes für Seeschifffahrt und Hydrographie“
werden Themen mit Dokumentationscharakter aus allen Bereichen des BSH veröffentlicht.
Durch die Publikation nimmt das BSH zu den Inhalten der Beiträge keine Stellung.
Die Veröffentlichungen in dieser Berichtsreihe erscheinen nach Bedarf.

WOCE Global Hydrographic Climatology im Internet:
www.bsh.de (Menü: Produkte → Bücher → Berichte des BSH)

ISSN-Nr. 0946-6010

C o n t e n t s

1. Introduction

To describe the mean of a state variable and its changes in a fluid such as the ocean or the atmosphere climatologies are used. The single variable should be representative, its precision stated and its changes statistically significant. The climatology in three or even four dimensions will describe parameter fields that should be physically meaningful. To describe a mean ocean circulation from those parameters will be misleading since there is never such a circulation: it is a statistically justified mean, only.

Therefore constructing a climatology has to take into account the underlying relevant physical processes and their scales in space and time. This in turn has implications on the sampling, or data coverage. To adequately cover a global ocean in view of the needs of a climatology will never be possible, or affordable. So the existing data base on the one side determines the temporal and spatial limits of a climatology, the formulation of the interpolation scheme its representativeness on the other .

Any ocean climatology will be a statistical artifact of an unadequately sampled changing fluid. But it is serving an important purpose: it is a reference data-set of the system and its variability. In view of the state of our knowledge about the slowly varying ocean today, such a reference serves well for supplying a bench-mark for a given and stated period to which one compares future data and their interpretation.

Discussing climate change needs to define in the above sense the “mean” and the low-frequency variability of the ocean. Only then can we measure changes and try to attribute these to either the natural variability or anthropogenic change.

The first climatology of the World Ocean by S. Levitus (1982) has become a common standard for the oceanographic community. Its profile and gridded data sets have been since widely used both by observationalists and modellers. The Ocean Climate Laboratory (OCL) of the US-NODC has since produced three improved versions of the 1982 climatology which appeared in 1994 (World Ocean Atlas 1994 (WOA94) (Levitus et al., 1994a-c)), in 1998 (World Ocean Database 1998 (WOD98) (Levitus et al. 1998)), and in 2002 (World Ocean Atlas 2001 (WOA01) (Conkright et al., 2002)).

Despite the overall success of the NOAA climatologies a number of deficiencies have been noted and need addressing. Thus, one of the main problems with the NODC/OCL climatologies is the production of artificial water masses. As Lozier et al (1994) have shown, averaging of oceanographic properties on isobaric surfaces results in the production of water masses which are not confirmed by the temperature-salinity diagrams of observed data. It has been suggested that averaging should be done on isopycnal surfaces which mimics the process of isopycnal mixing in the real ocean and does not produce artificial water masses. Gouretski and Jancke (1999) found a large degree of scattering of the deep temperature-salinity diagrams in the South Pacific, based on the WOA94 climatology in disagreement with high-quality data from the region. They also found that the High Salinity Shelf Water in the Pacific Sector was completely missing in the gridded climatology. Curry (2000) reported that both WOA94 and WOD98 climatologies omit information from the deepest samples resulting in the disappearance of features such as the deep western boundary currents.

A number of ocean climatologies for particular oceans and for the global ocean as a whole have been produced in the former Special Analysis Centre (WHP SAC) of the World Ocean Circulation Experiment (WOCE) Hydrographic Programme WHP Gouretski and Jancke, 1995, 1996, 1998). This centre was closed in 1999 but some of its activities have been continued by a group in the German Federal Maritime and Hydrographic Agency (Bundesamt für Seeschifffahrt und Hydrographie, (BSH)).

The WOCE Global Hydrographic climatology (WGHC) described in this report is intended to improve the quality, spatial and time resolutions and the geographical coverage compared to the first version of the global climatology produced in the former WHP SAC (Gouretski and Jancke, 1998).

2. Data basis

The data basis used for this study is composed of several data sets, which are described below.

2.1 World Ocean Database 1998 (WOD98)

The WOD98 database was used as a main data source for the study and contains about 1,5 million temperature-salinity profiles (Levitus et al., 1998). WOD98 consists of profile data from several oceanographic instrument types. Since both temperature and salinity data are needed for our analysis only the following data types were selected:

a) Ocean Station Data, referred to measurements made from a stationary ship. Temperature was measured by reversing thermometers, whereas seawater samples were gathered with special bottles,
b) Conductivity-Temperature-Depth (CTD) data, obtained by instruments, capable to measure pressure, temperature, conductivity and oxygen at a relatively high vertical resolution.

Compared with the previous version (WOA94) the WOD98 has been expanded considerably. According to Levitus et al. (1998) there is a much better data coverage in many years and regions since the publication of WOA94. Another improvement is a new duplicate checking scheme, which resulted in the elimination of ”near-duplicates” that existed in WOA94. After the publication of the WOA98 database, substantial amounts of additional historical data have become available, resulting in a new data base World Ocean Atlas 2001 (WOA01). However, this database was not available to us when the compilation of the WGHC climatology started.

2.2 WOCE data

The World Ocean Circulation Experiment (WOCE) has been a component of the World Climate Research Programme WCRP. This unique oceanographic experiment has set standards for making the essential high quality hydrographic observations on the global basis. Except for a few cruises, hydrographic observations during the WOCE were made between 1990 and 1998.

Though the total amount of the WOCE profiles is small compared with the whole content of the database used in this work, the WOCE Hydrographic Programme produced a data-set of unprecedented quality, which also substantially improved the data coverage for the deeper layers of the World Ocean. The total number of WOCE profiles obtained during the one-time and repeat hydrographic cruises included into the combined data-set amounts to ca. 9000 stations. Our subset of WOCE stations is more complete compared with that of the WOA01 dataset.

2.3 Other data

A number of data-sets have been acquired through other organisations and from individual scientists.

1) The German Oceanographic Data Centre (DOD, Hamburg) contributed with a substantial number of profiles obtained in the Atlantic Ocean aboard German research vessels,

2) The Alfred-Wegener-Institute (Bremerhaven, Germany) shared with us a collection of the data collected in the northern and southern polar regions,

3) The Arctic and Antarctic Research Institute AARI (Saint Petersburg, Russia) provided a unique data set from the western Weddell Sea (Weddell Ice Station Data),

4) The French Oceanographic Data Centre (IFREMER, Brest) contributed a number of French oceanographic cruises occupied in the Atlantic Ocean.

Among other data-sets, obtained in the earlier data-empty regions we mention a data-set from the Pacific sector of the Southern Ocean (Lamont Doherty Earth Laboratory, courtesy of S.Jacobs)

The total number of hydrographic profiles included in our composite data-set is 1,059,535 **(Fig.1)**

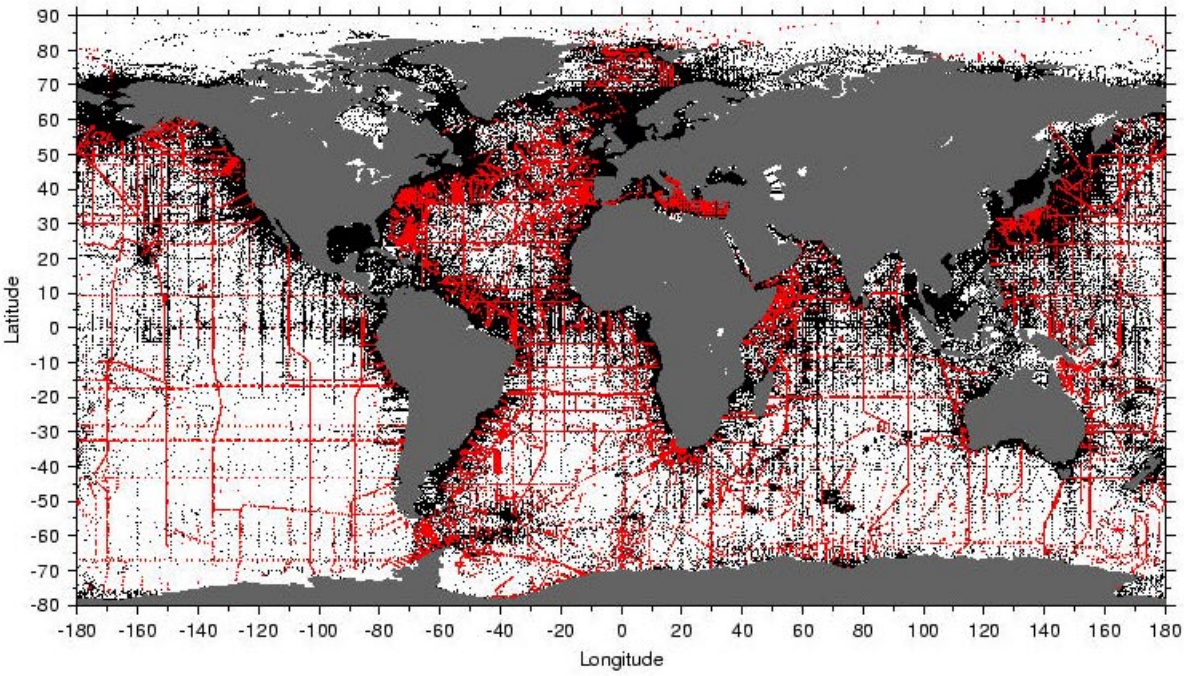

Fig. 1: Historical (black) and reference (red) profiles from the combined data set.

2.4 Subdivision into reference and historical data

As shown by Gouretski and Jancke (1999) based on a comprehensive data-set for the South Pacific, the accuracy of oceanographic measurements has changed considerably over the last decades, with earlier historical data exhibiting usually larger scattering and larger systematic biases. Therefore the selection of the historical data for the analysis is not exhaustive of the NODC CDROM data collection, but represents the data with the best quality indices as determined by a quality control procedure (Gouretski and Jancke,1999) briefly outlined in Section 3. Based on this data quality assessment a composite data set **(Fig.1)** was divided into two subsets, to avoid simultaneous treatment of data of substantially different quality:

a) **A reference data set**, comprising high quality cruises occupied after 1970 (a total of 19867 profiles distributed over 384 cruises).
b) **A historical data set**, comprising older cruises occupied mostly before 1970 as well as profiles not included into the high-quality subset (a total of 1039668 profiles distributed over 41757 cruises).

WOCE data provided the basis for the high-quality reference data set. The reference data-set includes also high-quality non-WOCE data. Though the total number of high-quality profiles is an order of magnitude less compared with the historical data, the high-quality profiles provide a *reference* against which the historical data are validated. The reference dataset was compiled for the study of systematic offsets in the hydrographic data and is described in details by Gouretski and Jancke (2001).

2.5 Time- and spatial distribution of the data

The depth coverage of the hydrocasts (e.g. the ratio of the last observed depth to the local bottom depth) is shown in **Fig. 2.** The coverage is better for the shallow regions of the ocean, whereas below about 1500 meters historical hydrocasts on average extend only to the ocean mid-depth.

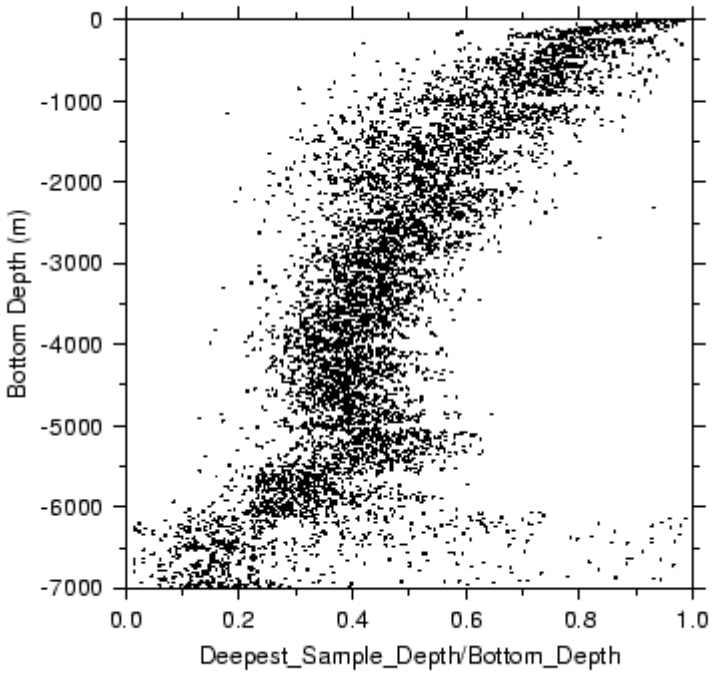

Fig. 2: Average ratio of deepest sample depth to bottom depth versus sample depth.

The average vertical distance is given between the neighbour water samples (**Fig. 3)**. Historical profiles have generally a rather poor vertical resolution, with distances between samples exceeding 400 meters for depths below 1500 meters. Results depicted in Fig. 3 were used to compromise on the maximum "gap" size between the bottles of the cast allowing a vertical interpolation of water properties. Most of the data were obtained between

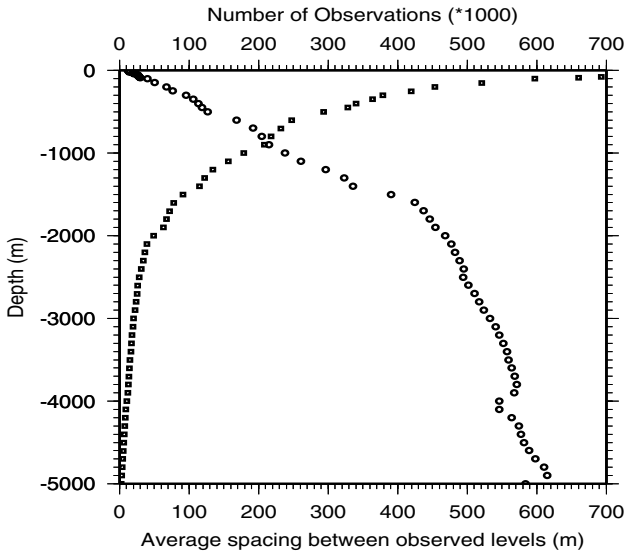

Fig. 3: Average spacing between observed levels versus sample depth.

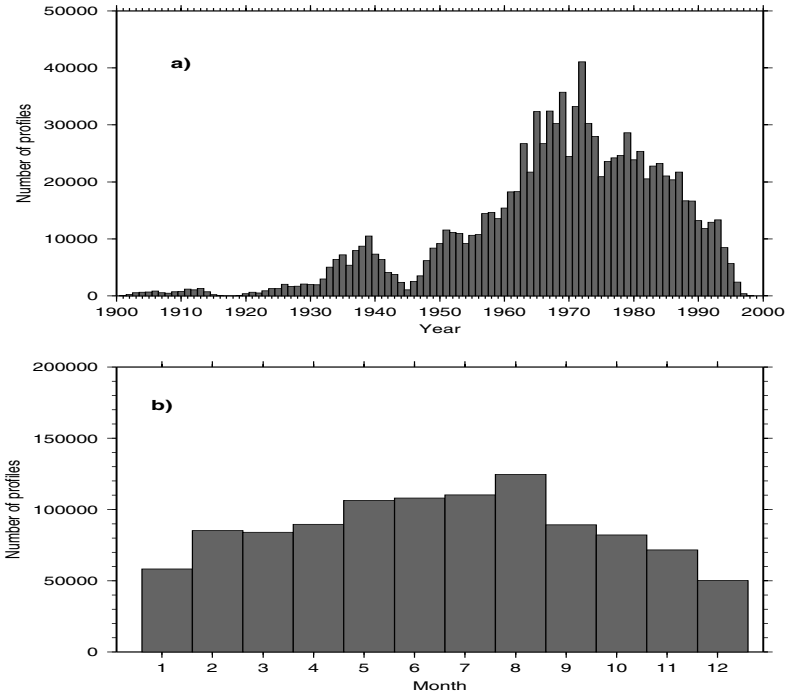

Fig. 4: Number of profiles per year (a) and per month (b).

1960-1990 (**Fig. 4a**). An apparent decrease of the data acquisition rate during the last decade is explained by the lag between the data acquisition and its availability to the oceanographic community. The overall sampling is biased to the summer period of the Northern Hemisphere (**Fig. 4b**).

3. Data Quality Control

3.1 Cruise identification

The quality analysis procedure used in the study requires a cruise identification of the data. Unfortunately, in many cases the NODC collections still do not provide information to link the data to a particular oceanographic cruise occupied by one and the same ship. The historical profiles of the composite data set, selected for the analysis are distributed among about 10000 NODC archive codes, which often are linked to the data from many different cruises of one and the same ship. Within each NODC archive cruise number all profiles were ordered by time, and a time demarcation between a pair of new ”cruises” was set as soon as the time span between two consecutive stations exceeded 7 days. This time separation criterion was set rather arbitrarily, and it does not exclude the possibility when the time separation of 7 or more days occurred within one and the same hydrographic cruise, or when the gap between the two cruises was less than a week. As a result, all selected hydrographic profiles were ascribed to a total of 41757 new cruises.

3.2 Random errors

Evolution of measuring technique and methods along with very different quality standards caused a high degree of inhomogeneity of the historical hydrographic data set and invoked a large literature devoted to the problems of quality control of oceanographic data. Most of the quality control procedures (Levitus et al., 1994; Olbers et al., 1992; Curry, 1996; Gouretski and Jancke, 1999) were aimed to identify *random* errors in the data.

The quality evaluation of the composite dataset used in this study benefited from the fact that all of the source data had already been validated to a certain degree. A description of the validation procedure applied to the WOA01 data was given by Levitus et al. (1994) and Conkright et al. (1994). All WOCE data have been checked for their quality both by respective principal investigators and (in many cases) by independent experts. However, the investigation of the historical hydrographic data quality for the South Atlantic (Gouretski and Jancke, 1995) and for the North Atlantic (Lozier et al., 1995) showed that some highly questionable data from the WOD98 database obviously passed through the quality checks implying the necessity of a more rigorous quality control.

In order to further validate the data we used a method developed by Gouretski and Jancke (1999) and tested for the South Pacific historical data set. Quality checking is done in the density-parameter space. The method is based on the experimental fact that relations between potential temperature (or density) and other parameters are locally well defined in the World Ocean and are relatively tight below the thermocline level. The density-parameter curves for a group of neighbour stations is approximated by vertical subdivision into small density bins and connection of mean points for each bin with straight lines. Then mean values and standard deviations of parameters from the mean curve within each bin are computed and any value differing by more than some prescribed number of standard deviations (2.5 in our case) from the mean curve is rejected (flagged).

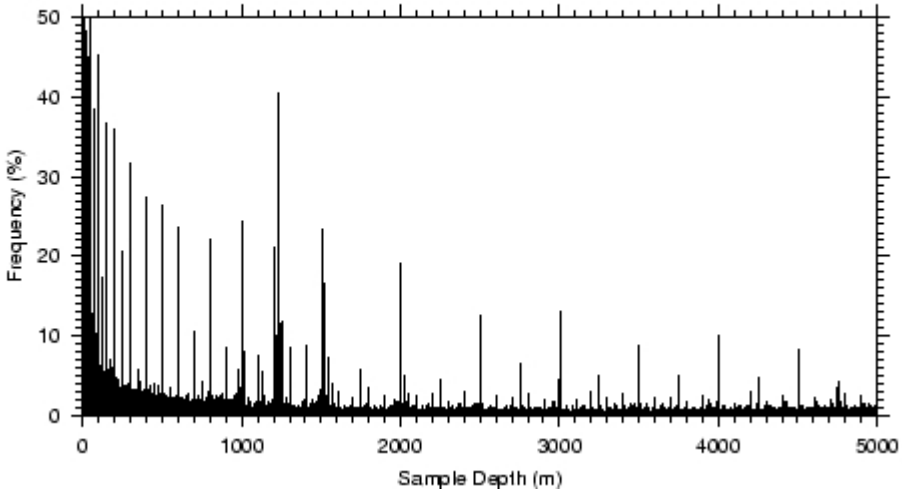

Fig. 5: Frequency distribution of the sample depth.

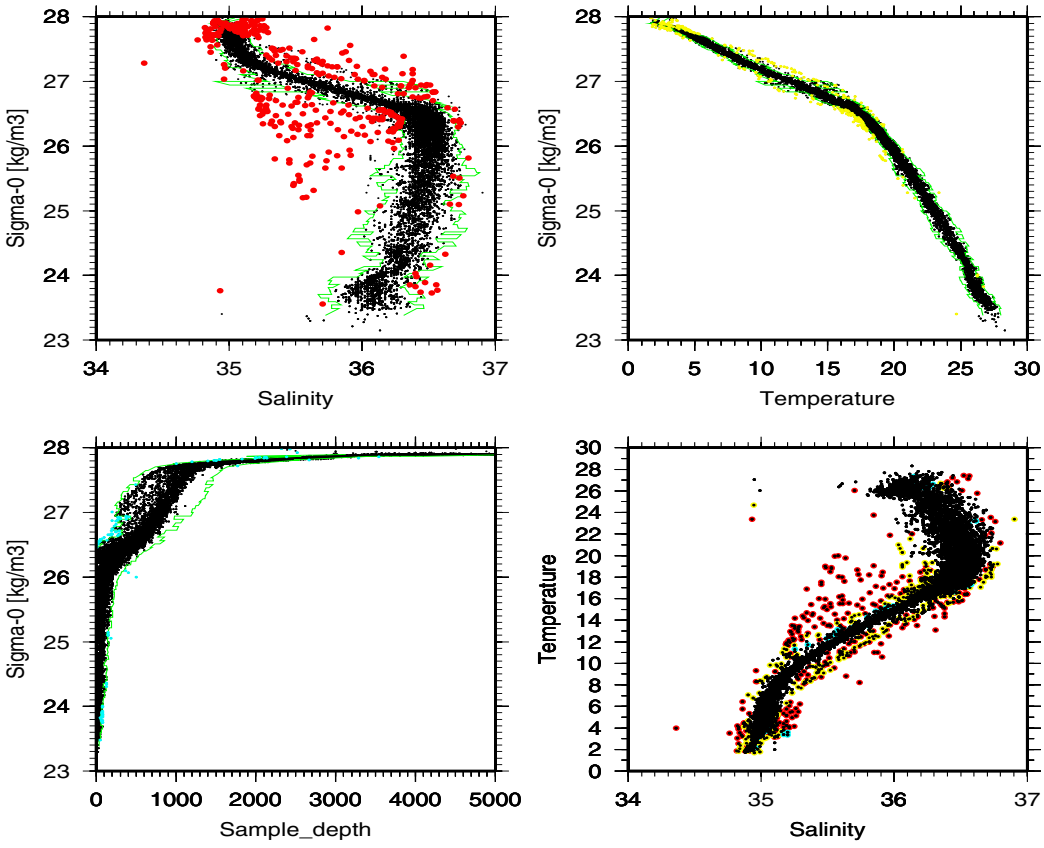

Fig. 6: Example of the statistical quality control. Rejected observations are shown in red (salinity check), yellow (temperature check), and green (sample depth check)

Depending on the spatial distribution of the data the size of the geographical box within which a mean density-parameter relation is assumed to be spatially invariant varied between 111 km by 222 km and 333km by 666 km.

Eight parameters were subjected to quality control: potential temperature, salinity, oxygen, silicate, nitrate, phosphate, ratio [NO]/[PO]. Since every density value (determined by T and S) is characterised also by the depth of the respective isopycnal, the depth of the T-S pair falling within a density bin was also checked as an independent parameter. The following explains the inclusion of the statistical check for the sample depth.

Before the introduction of CTD-type probes, which measure pressure (depth) with an accuracy of about 0.1%, a common oceanographic practice was to estimate depth by means of wire length and angle between the bottles. The bottle trip depth was (sometimes) determined by means of pairs of protected/unprotected thermometers attached to some deep bottles. For a considerable number of historical casts unprotected thermometers were

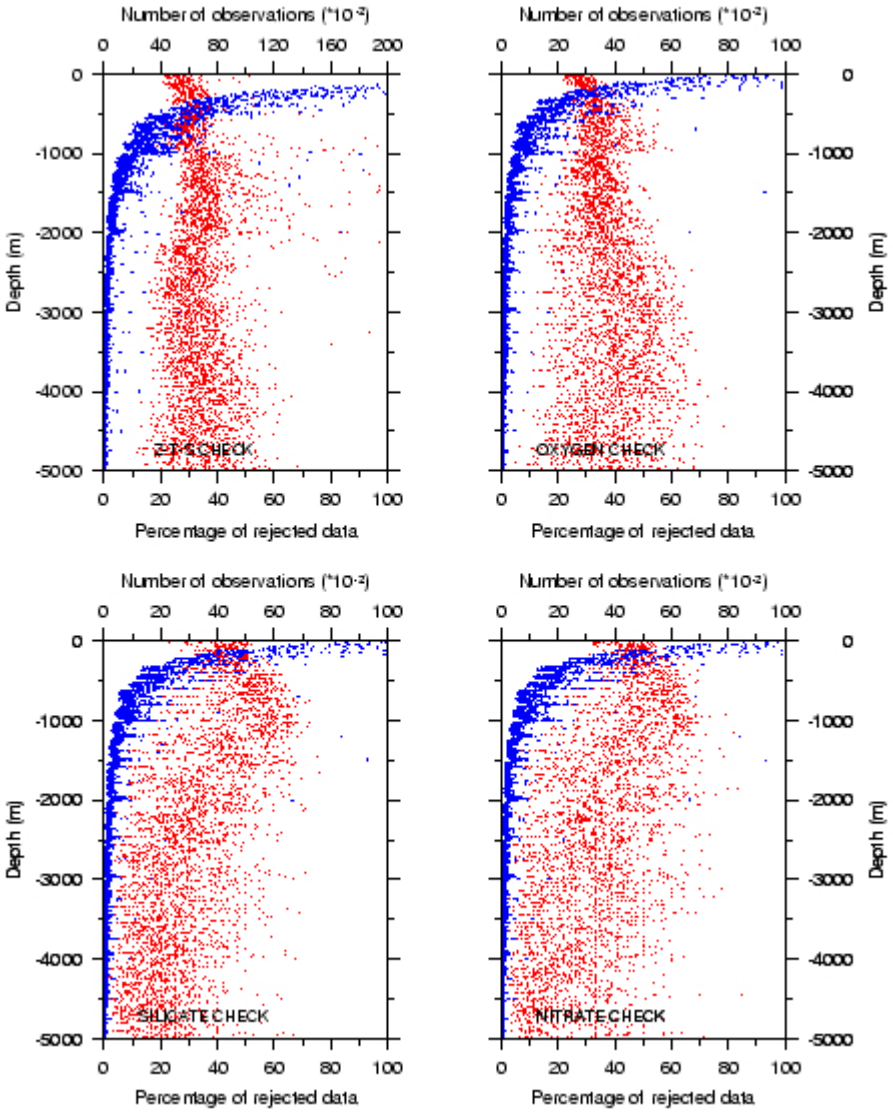

Fig. 7: Percentage of rejected observations (red) and a total number of observations (blue) versus depth. Depth bin width is 1 meter.

not used or their number was insufficient to determine the depth of each sample. The frequency distribution of sample depth is depicted in **Fig. 5** and demonstrates that

observations tend to cluster at some ”standard” levels. Since older oceanographic techniques were not conducted to meeting target depths, the spikes on the histogram may indicate target depth rather than those actually sampled.

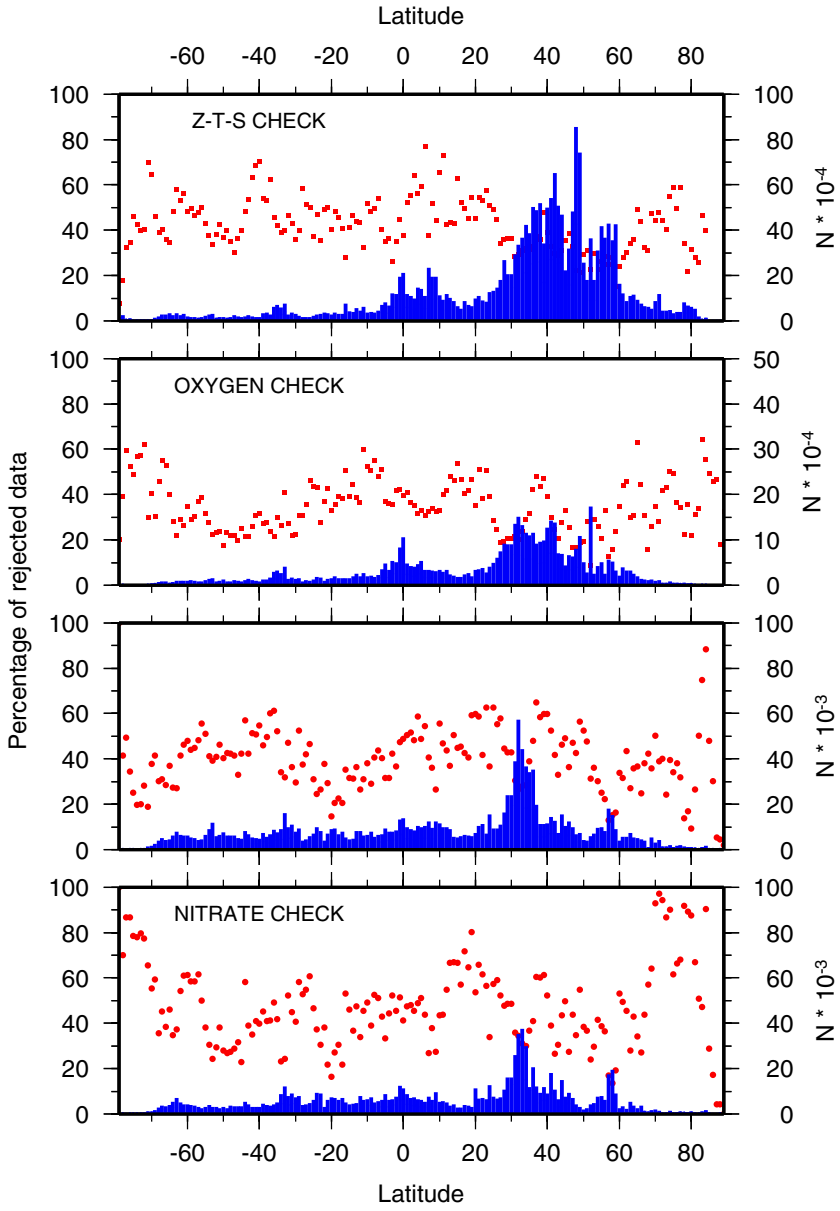

Fig.8: Percentage of rejected observations (red) and number of observations in 1-degree latitude zones (blue).

An example of our quality check for the area 100-110°E 30-20°S in the Pacific Ocean is shown in **Fig.6**. The procedure described above effectively removes outliers. Thus, a couple of profiles with obviously erroneous sample depths could not be identified as outliers by the statistical check for T and S only, but were rejected by the statistical check on sample depth. The statistical check was repeated three times. Each time the percentage of outliers per cruise was computed. A certain fraction of cruises was found to have a much higher percentage of rejected observation. Such cruises were flagged and excluded from the further analysis. The percentage of rejected observations (**Fig. 7**) varies with depth,

depending on the number of observations at a depth level, spatial distribution of the data, data quality and natural variability. The percentage of rejected observations per one-degree latitude zone is given in the **Fig. 8**.

There exists a clear decrease of percentages of rejected observations for each parameter with time (**Fig. 9)**. This indicates improvements in observational instruments and methods. The data from the 1990s (the main operational phase of WOCE) are characterised by the lowest percentage of outlier.

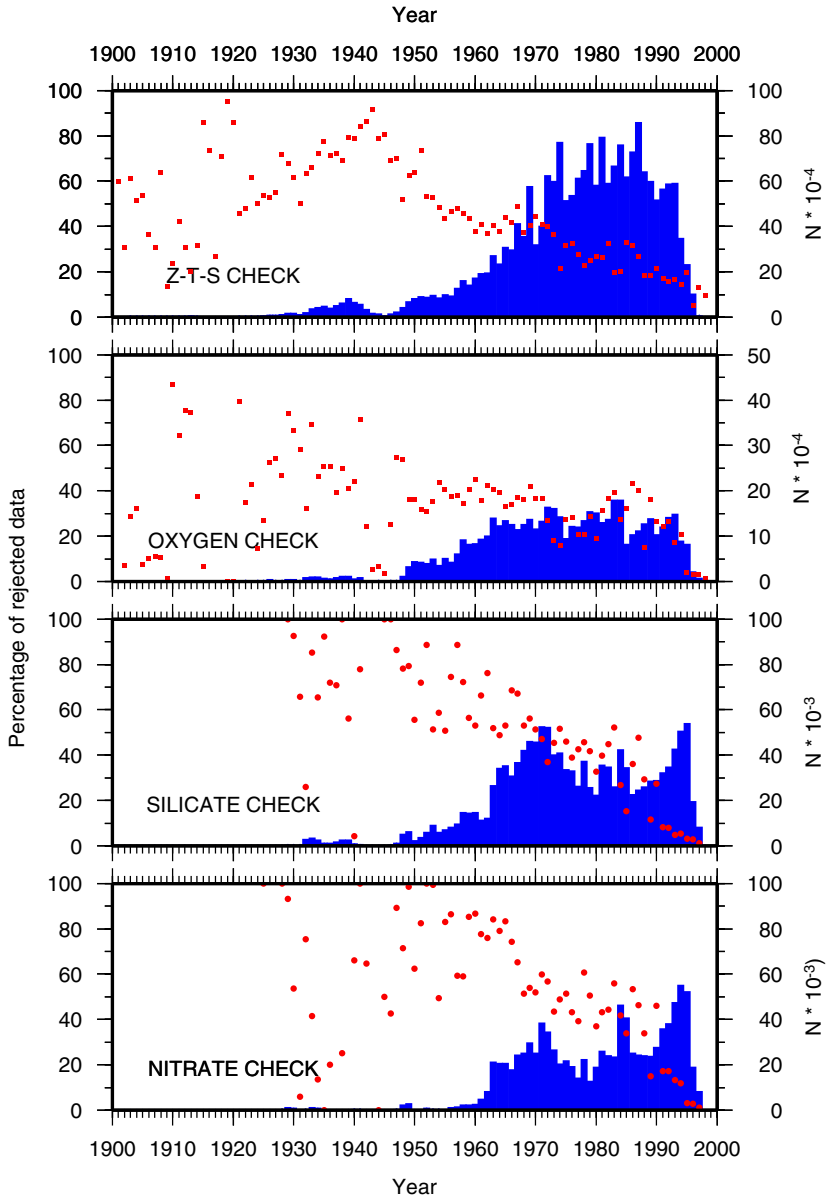

Fig. 9: Percentage of rejected observations versus year (red) and the number of observations per year (blue).

3.3 Systematic errors

The problem of estimating systematic errors in the data was not properly addressed until recently. Identification of *systematic* errors was usually made at the stage of the subjective

(expert) quality control. In areas with sparse data coverage systematic errors often manifest themselves as strong local features, which are identified by a proper control of property distribution maps or temperature-parameter diagrams. Substantial improvements in the observational techniques and methods reduced significantly measurement errors, but, on the other hand, stressed the importance of estimating systematic differences between the data when merging data of different origin. Differences in observational techniques and methods are the main cause for systematic errors (offsets) in the data, as soon as a composite data base is considered. CTD-systems have increasingly replaced Nansen bottles since the mid-1960s, accompanied by a replacement of the titration method by conductive salinometers. Manual methods for nutrient determinations have been replaced by automated methods, and the method for titrating oxygen samples changed in the late 1950s. A brief description of the possible causes for inter-cruise offsets is given below.

Salinity. Among commonly measured oceanographic parameters salinity is the only parameter whose measurement can be referenced to a common standard, i.e. IAPSO Standard Seawater (SSW). However, a number of factors lead to systematic errors in salinity measurements such as (1) different bottle types, (2) time lag between water sampling and salinity determination, (3) offsets between different batches of IAPSO Standard Sea Water, (4) salinometer response shift, (5) differences between up and down cast values because of the hysteresis in pressure, temperature or conductivity sensors.

Oxygen. The method for titrating oxygen samples changed in the late 1950s. Though some corrections to the older data have been proposed (Worthington, 1976; Gordon and Molinelli, 1982) problems with oxygen data forced Lozier et al. (1995) to eliminate pre-1960 data completely from the database. Culberson et al. (1991) compared results of four scientific groups and noted two main sources of errors in oxygen determination: (1) the concentration of dissolved oxygen in the reagents and (2) the value of the seawater contribution to the blank. The analytical methods used to determine dissolved oxygen employ volumetric techniques and give the amount of oxygen per unit volume of seawater. Transfer to the weight concentration requires knowledge of the temperature of the seawater at the time of sampling and it was not routinely measured in the past. According to Culberson et al (1991) a 25^{o}C difference between the sampling and assumed temperatures may result in 0.5% error in the weight oxygen concentration.

Nutrients. Problems with the unsatisfactory quality of nutrient data are also well known. Nutrient scatter diagrams usually exhibit rather dispersed clouds of points, where other more precisely measured parameters reveal tight temperature-parameter relationships. One of the major concerns with respect to the nutrient data is whether measurements made using manual methods may be combined with measurements made using automated methods. Another source of discrepancies was found to be due to problems in the standardisation procedures used by different laboratories. A thorough treatment of random errors and biases in nutrient determinations was given by Holley (1998), who divides factors affecting precision and accuracy of nutrient measurements into four problem areas:

(1) *Instrument, mechanical and chemical factors.* These include refractive index problems, bubble production and its effect on mixing, the contamination of a sample, drift within a run due to changes in the reagent, and differences in the sample wash time.
(2) *Standardisation.* The working calibration standards differ between laboratories by type, supplier, batch, quality, and preparation technique. Standards prepared in low nutrient sea water are less stable than in distilled or artificial sea water due to the organisms present.

3.4. Calculation of inter-cruise offsets

A very important improvement relative to the WOA94 and WOD98 and WOA01 climatologies is the treatment of systematic errors in the data. Such error (or biases) were determined through the analysis of the inter-cruise property offsets. The method was

successfully applied to an earlier version of the data-set used in this work. For a detailed description we refer to Gouretski and Jancke (2001), and below is given only an overview of the method.

The procedure starts with the estimation of inter-cruise property offsets within cross-over areas. The size of the crossover area and the potential temperature and depth ranges were specified based on the estimate of parameter variability on potential temperature surfaces. The size of the crossover area was limited by 300 km, and only samples below 800 meters and colder than 3^{o}C were taken for the inter-comparison. For each pair of intersecting cruises/sections the inter-cruise offset is calculated as the average of individual profiles. Errors in temperature are neglected. A number of geographical areas with extremely high variability within the deep part of the water column were excluded (e.g. Irminger and Labrador Sea, Antarctic continental slope).

Gouretski and Jancke (2001) suggested a decomposition of observed inter-cruise offsets D into systematic and non-systematic components. For each pair of cruises (i,j) the observed offset is:

$$D_{ij} = \Delta_{ij} + n_{ij}, \qquad (1)$$

where $\Delta_{ij} = \delta_i - \delta_j$ is the *true offset*, e.g. the part of the inter-cruise offset due to systematic errors δ in the data, whereas n_{ij} represents the non-systematic part of the offset, caused by random errors and by the combined effect of the time-space variability within the cross-over area.

3.5. Calculation of biases for reference cruises

Typically, for a set of *N* cruises the number of the offset estimates M >> N (M is the number of crossover areas). The set of equations (1) may be written in the general standard form :

$$\boldsymbol{E\delta + n = D}, \qquad (2)$$

where in the present case, solution, noise and offset vectors are:

$$\boldsymbol{\delta} = (\delta_1, \delta_2, ., ., \delta_N) \qquad (3)$$

$$\boldsymbol{n} = (n_1, n_2, ., ., n_N) \qquad (4)$$

$$\boldsymbol{D} = (D_1, D_2, ., .,D_M). \qquad (5)$$

For a pair of cruises *(p,q)* elements of the *k*-th row of the matrix ***E*** are:

$$E_{kl} = \begin{cases} 1 & \text{for } l = p, \\ -1 & \text{for } l = q, \\ 0 & \text{for } l \neq p,\ l \neq q \end{cases} \qquad (6)$$

Thus, the M equations (2) are used to estimate *N* values δ_i and *M* values n_i, or *M*+*N* altogether. The solution of the system is obtained in a root-mean square sense (Wunsch, 1996):

$$\boldsymbol{\delta=(E^TE)^{-1}E^TD}; \qquad (7)$$

For the reference data set the system of equations (2) was solved to get the reference cruise biases δ. Since no true reference data is available, we subtracted the average of all WOCE biases from each individual bias after the root-mean-square solution of (11) was obtained. The

total number of equations (cruise pairs) was of 2094, 665, 404, 331 and 331 for salinity, oxygen, silicate, nitrate, and phosphate respectively, with systematic biases δ determined for 384, 213, 145, 133 and 136 cruises.

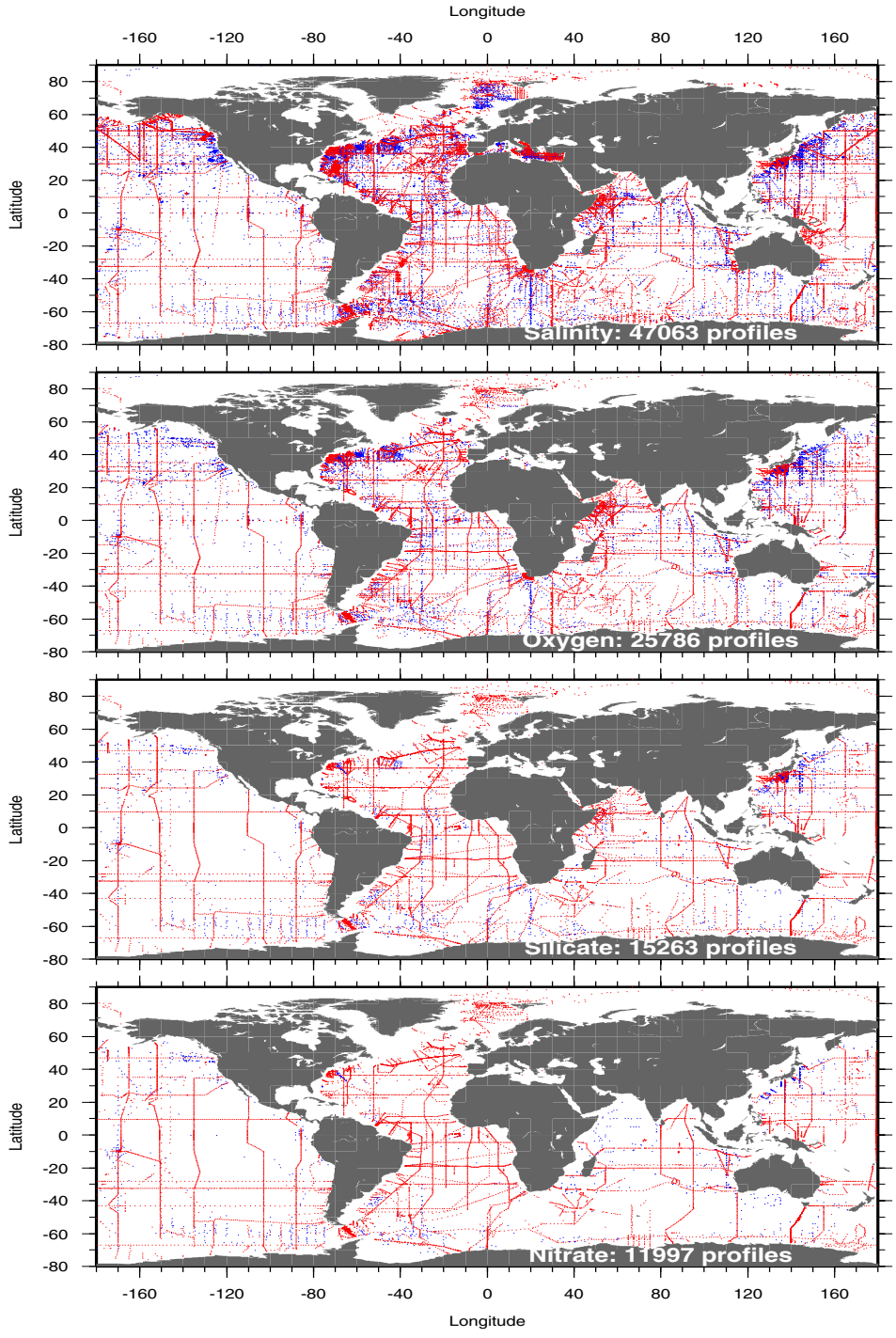

Fig. 10: Adjusted reference (red) and historical (blue) profiles.

Multiplicative scale factors were calculated for oxygen and nutrients unlike additive corrections (biases) for salinity. As equation (2) deals with additive biases, the observed crossover differences D_{ij} for oxygen and nutrients which were respectively recalculated for "standard" nutrient concentrations. There are several reasons to use multiplicative factors instead of biases. One reason is that multiplicative scale factors help to avoid negative nutrient/oxygen

values for very low near-surface concentrations (see a more detailed discussion in Johnson et al., 2001).

3.6 Calculation of biases for historical data-set

Whereas biases for the reference cruises were obtained by solving (2), biases for *historical* cruises were calculated relative to the reference cruises, corrected for systematic errors.

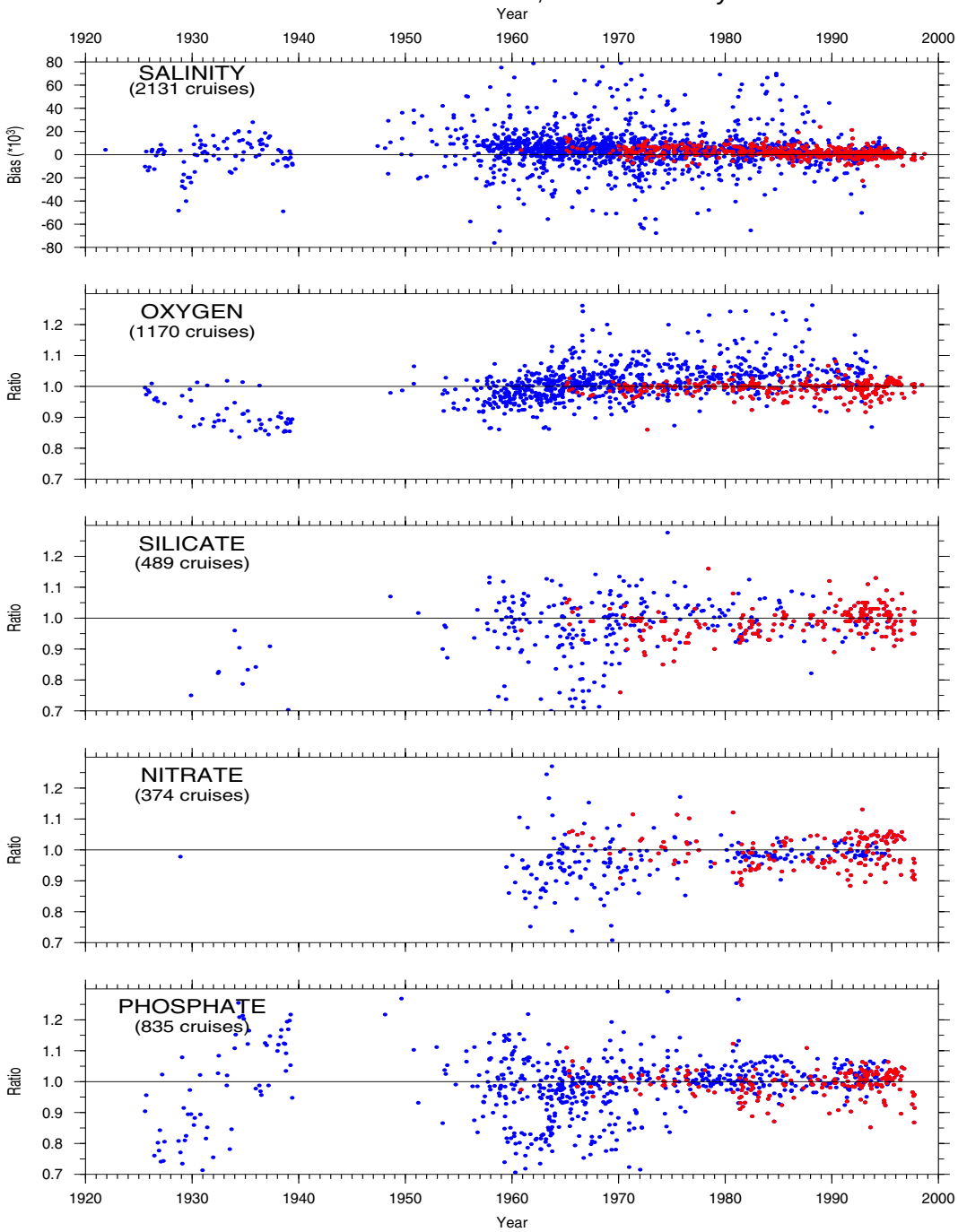

Fig. 11 Cruise biases versus time (red – reference cruises, blue – historical cruises).

Much fewer deep water samples are typically available for the historical data. In order to get a sufficient number of samples for statistically meaningful estimates, the maximum station separation was increased to 400 km (compared with 300 km for the high-quality data set) with

the minimum of 10 station pairs, required for the offset estimate. For each historical cruise property biases were calculated as the average of individual offsets relative to reference stations within the respective crossover area. For all parameters historical cruise biases exceed considerably those for the cruises of the reference data-set (**Fig.10).**

Particularly large biases for some historical cruises are indicated in **Fig. 10**. For example, most of the data from the 1930s were obtained during the expeditions of the R/V *Discovery* in the Southern Ocean. These data are highly biased in oxygen by 0.5- 0.6 ml/l, and in silicate (15-50 μmol/kg). Another problem with historical data is a large scattering of individual profile offsets within the cruise. We decided therefore to apply individual profile bias corrections instead of a cruise average correction.

The spatial distribution of adjusted profiles is shown in **Fig. 11** for all parameters. The coverage of available high-quality cruises made it possible to calculate biases for a total of 71776 historical profiles.

4. Interpolation onto a regular grid

4.1 Optimal interpolation method

The optimal interpolation method was used to compute climatological property distributions of the selected standard levels on a regular grid. The methodology we use in this study has been described previously in the oceanography literature, where it is variously referred to as Gauss-Markov, optimal or statistical interpolation, or objective analysis (Gandin, 1963; Bretherton et al., 1976). The technique is commonly used to interpolate irregularly sampled, noisy data onto regular grids for subsequent analysis.

The method employs a location-dependent background or first-guess field *G*. An analysed grid-point value F_o is the first guess evaluated at the grid point plus an interpolated analysis error. The latter is an interpolation to the grid-points of the differences between observation values and values of the background field at the observing points. Thus an analysed grid-point value F_o is:

$$F_o = \sum w_i(F_i - G_i) + G_o.$$

The weights w_i are those weights which minimise the ensemble average of the squared difference between the analysis value and the true value of the field signal. For any specific set of observing sites *(i,j)* and grid-point *(o)* locations the first-guess-minus-observation differences and the grid-point first-guess error are considered to be stochastic variables with a joint statistical distribution for which the covariances are known or can be computed or modelled.

The minimisation gives a set of linear equations for optimal weights $\boldsymbol{w}$:

$$(\boldsymbol{A} + \lambda \boldsymbol{I})\, \boldsymbol{W} = \boldsymbol{\rho} \qquad (1)$$

where **A** is the signal correlation matrix with elements $A_{ij} = \rho(\Delta x_{i,j})$, $\boldsymbol{I}$ is the identity matrix, and $\lambda = \sigma_n^2/\sigma_f^2$, an $\Delta x_{i,j}$ represent the spatial separation between points i and j, $\boldsymbol{\rho_i} = \rho(\Delta x_{i0})$.

The method requires knowledge of variances of signal and noise and of the spatial autocorrelation function $\boldsymbol{\rho}$ for *increment* fields. The signal is defined as variability with scales larger than the smallest scales of interest. The noise is variability with smaller scales, plus random instrumental errors.

An advantage of the optimal interpolation method is that it also returns an estimate of the uncertainty (error variance). The relative error ε' depends on the observation locations, and on the levels of signal and noise variance:

$$\varepsilon_0' = (1 - \Sigma\Sigma\, \rho_{oi} A^{-1}_{ij} \rho_{oj}), \qquad (2)$$

Another important advantage over empirical distance-weighting schemes is that the optimal interpolation method takes into account relative separations among the observing sites but not only the individual separations between the grid-point and the observing sites. The presence of the correlations among input increments in the weight determination algorithm controls for redundancy of information from sources whose increments are statistically related.

4.2. Data reduction

The optimal interpolation requires inversion of the covariance matrix, which becomes impractical for a large number of observational points. Usually, only the data points closest to the grid node are taken to obtain a field estimate. It means, that most of the observed data are actually lost for the analysis. In this case the climatic estimate is based on a number of observations which may not be representative of the regional long-term mean conditions.

Chelton and Schlax (1991) analysing colour scanner satellite data introduced the notion of time averaging to the standard optimal interpolation method in recognition that some temporal averaging is desirable to reduce the aliasing of high-frequency variability in the signal. Time of observation is neglected in our interpolation and original data are subject to spatial averaging prior to optimal interpolation. The ocean was subdivided into 0.5-degree latitude zones between 80°S and 90°N. Each zone was in turn subdivided into boxes with the longitude size equal to 55 km for the zone mid-latitude. Thus the quantity that is estimated is not the signal at a particular estimation point but its average over a 55x55 km box. Data averaging was done within each box if at least 4 profiles were available. Similar averaging procedure was used by Levitus (1982) and in the later updates of the NOAA ocean climatology, where one-degree data averages served as input for the further analysis. However, unlike in NOAA climatologies we performed averaging on the potential density surfaces, referenced to the pressure of the respective standard level. Since diapycnal processes are assumed to be important in the near-surface layer, within the upper 100-meter layer averaging was performed on the isobaric (standard depth) surfaces.

The averaging results in a 10-fold reduction of the input data, from 1,059,535 original profiles to only 106 330 profiles (for all data mean averaging), with the total number of the box-averaged profiles being 21311. **Fig. 12** shows the distribution of the averaged and original profiles used finally for the optimal interpolation of temperature and salinity.

4.3. Modelling spatial lag correlation

The correlation structure for the increment field has a central and highly sensitive role in the optimal interpolation method. The optimal interpolation requires the knowledge of the spatial correlation function ρ, and the signal-to-noise ratio γ^{-1}. Unfortunately, because of a general data paucity the determination of the spatial correlations for the fields of oceanographic parameters is a difficult task, compared with the situation in meteorology, where time series observations are often routinely available. Satellite observations however provide sufficient information to determine statistical characteristics of oceanographic fields but only at the ocean surface (Kuragano and Kamachi, 2000). Repeat XBT sections were also used to infer the spatial correlation structure. Meyers et al (1991) give an example of space-time scale

determination of sea surface temperature and depth of the 20°C isotherm in the Tropical Pacific Ocean.

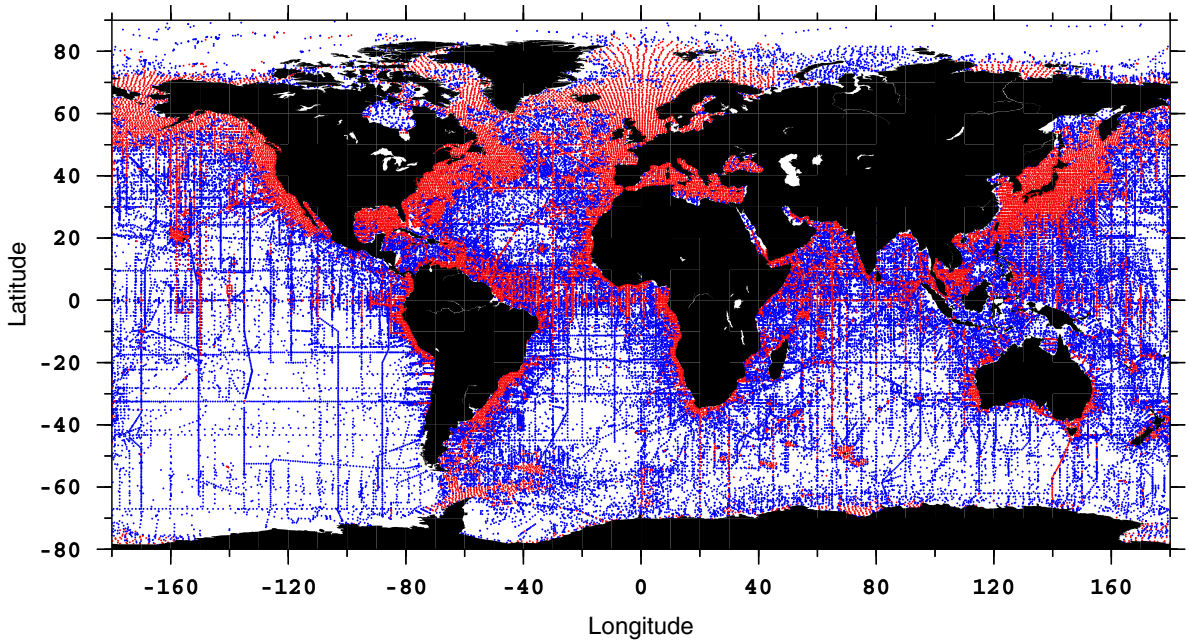

Fig.12: Observed (blue) and averaged (red) T,S-profiles used as input for the optimal interpolation.

In most applications of optimal interpolation the negative squared exponential (called often "Gaussian function") has been favoured as the shape of the correlation function, although many other functions have been considered. A "gaussian" model of the autocorrelation function was used for this study, which employs a decorrelation length scale *R:*

$$\rho\,(r) = exp\,(-r^2/R^2) \qquad (3)$$

We note, that our assumption of this covarience is highly arbitrary, and we choose the "Gaussian" form because of the relatively simple structure as well as the lack of a more appropriate choice. The parameter *R* (decorrelation scale or e-folding length scale) is a measure of the spatial scale of correlation. The shortcomings of the "Gaussian" function when applied to a typical geophysical data can be summarised as a propensity to overestimate the weights at short lags and underestimate them at large lags (McIntosh, 1990). This amounts to oversmoothing at small scales and may be countered by artificially lowering the value of λ, causing the interpolation to follow the data more faithfully.

It is well known, that many important features of the oceanic circulation and water mass distribution are closely connected to the bottom topography. Thus, most of the World Ocean boundary currents are situated above the continental slope, having a cross-current scale of o(50km), e.g. small compared with the typical size of the ocean basin. Similar, fresh water river plumes significantly alter property distributions in the coastal areas, but are effectively separated from the open ocean areas by sharp fronts. It is therefore desirable to preserve the "narrowness" of boundary currents in the analysed fields. Using large decorrelation scales would result in unrealistically wide boundary currents. We included the topographic information into the calculation of the characteristic length scale *R*. For each grid node the distance *D* between the node and the coast was determined, with the respective *R* determined from:

$$R = R_{max} \;\; for \;\; D >= D_{max,}$$

$$R = R_{min} + (R_{max}-R_{min})\cdot D/D_{max} \quad \text{for} \quad 0 < D < D_{max} \qquad (4)$$

where R_{min} is the e-folding scale at the coast line *(D=0),* and R_{max} is the maximum e-folding length scale in the open ocean. The spatial correlation scale R_{max} is set as 450 km in our calculation and is intended to represent typical signal scales, D_{min} is set as 500 km. The spatial distribution of the decorrelation length scale is given in **Fig.13.**

4.4. Computational details

A set of 45 standard levels was selected for which the objectively analysed property fields were computed:

0, 10, 20, 30, 40, 50, 75, 100, 125, 150, 175, 200, 250, 300, 350, 400, 450, 500, 600, 700, 800, 1000, 1100, 1200, 1300, 1400, 1500, 1750, 2000, 2250, 2500, 2750, 3000, 3250, 3500, 3750, 4000, 4250, 4500, 4750, 5000, 5250, 5500, 5750, 6000 meters.

We note that the NOAA climatologies are available for 33 levels for the depth range 0-5500 meters.

For each grid point, data are initially selected in a large subdomain, whose radius is arbitrary set as 750 km (about 2 times larger than the space correlation scale). The first-guess field estimate is taken as the mean of the data in the subdomain. Next, data are selected for the objective mapping: inside a subdomain up to 150 nearest observations are retained

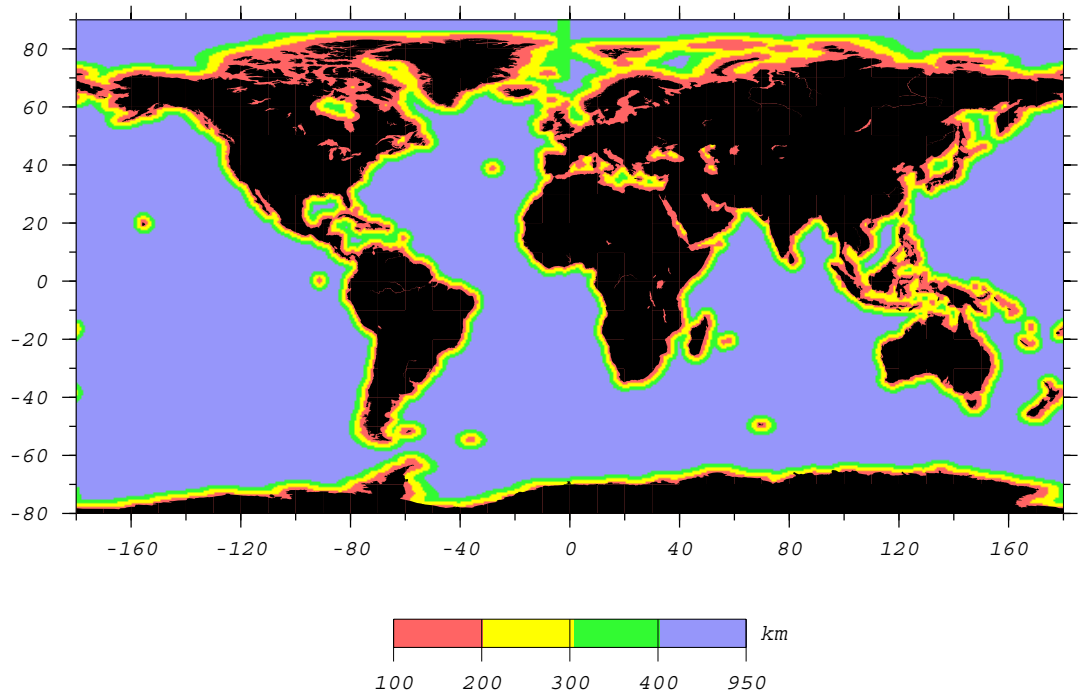

Fig. 13: Decorrelation length scale (km).

To avoid averaging of the data from basins essentially separated from each other optimal interpolation was done for a number of oceanic basins or coastal areas. These interpolation areas are shown in **Fig. 14**.

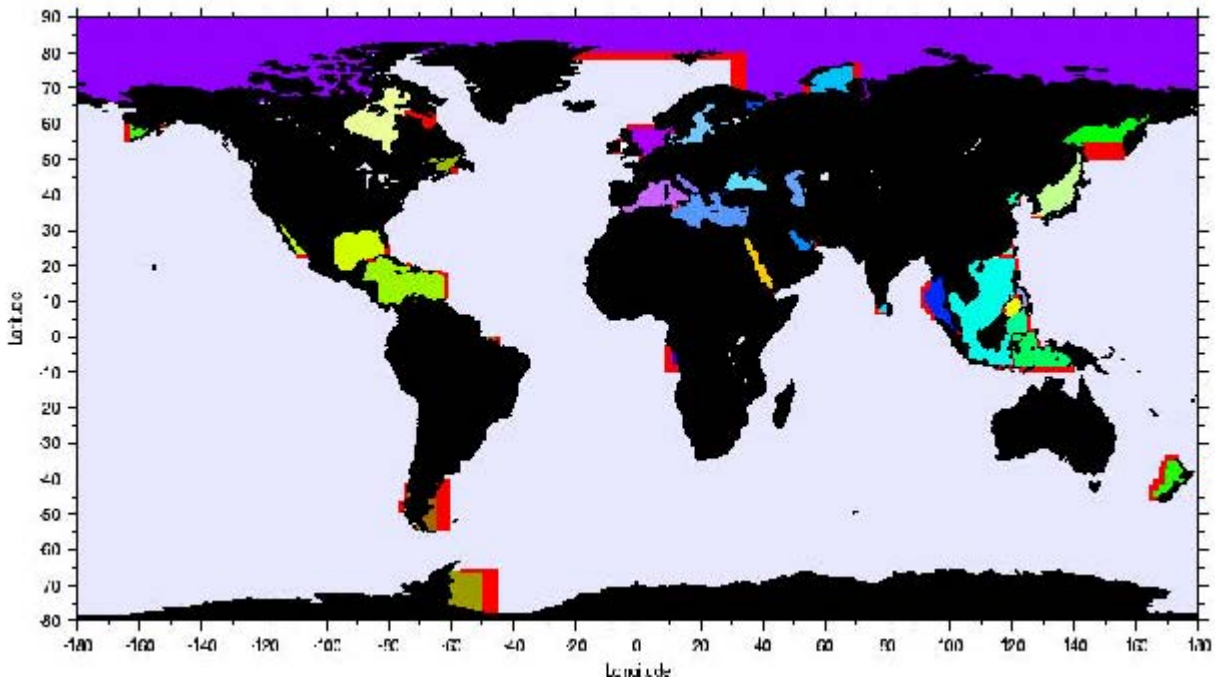

Fig. 14: Interpolation areas. Overlapping areas are shown in red.

Property distributions at the 200 meter level **(Fig. A1a-b)** and near the bottom **(Fig. A1c-d)** are given in the Appendix . Also shown are property standard deviation calculate on isopycnal surfaces **(Fig A2).**

5. Comparison with WOA01 climatology

This technical report is not intended to provide a detailed description of the differences between the present and WOA01 World Ocean climatology. However, we want to provide the reader with some results of our inter-comparison in order to explain and document improvements achieved through the application of our methods of data quality control and interpolation.

The main differences between the present and the WOA01 climatologies are due to differences in the (1) data basis, (2) quality control procedure, (3) treatment of systematic errors, and (4) spatial interpolation scheme. The data basis used for this study was extended through the incorporation of a number of high-quality data-sets. This is important for such data poor areas, as central parts of main ocean basins, especially in the South Pacific Ocean. The quality control procedure used in this study provides a more elaborate tool in identifying erroneous observations by estimating the quality of particular cruises. An important deviation from the WOA01 climatology is the treatment of systematic biases (errors) in the data, which were calculated relative to the reference WOCE dataset.

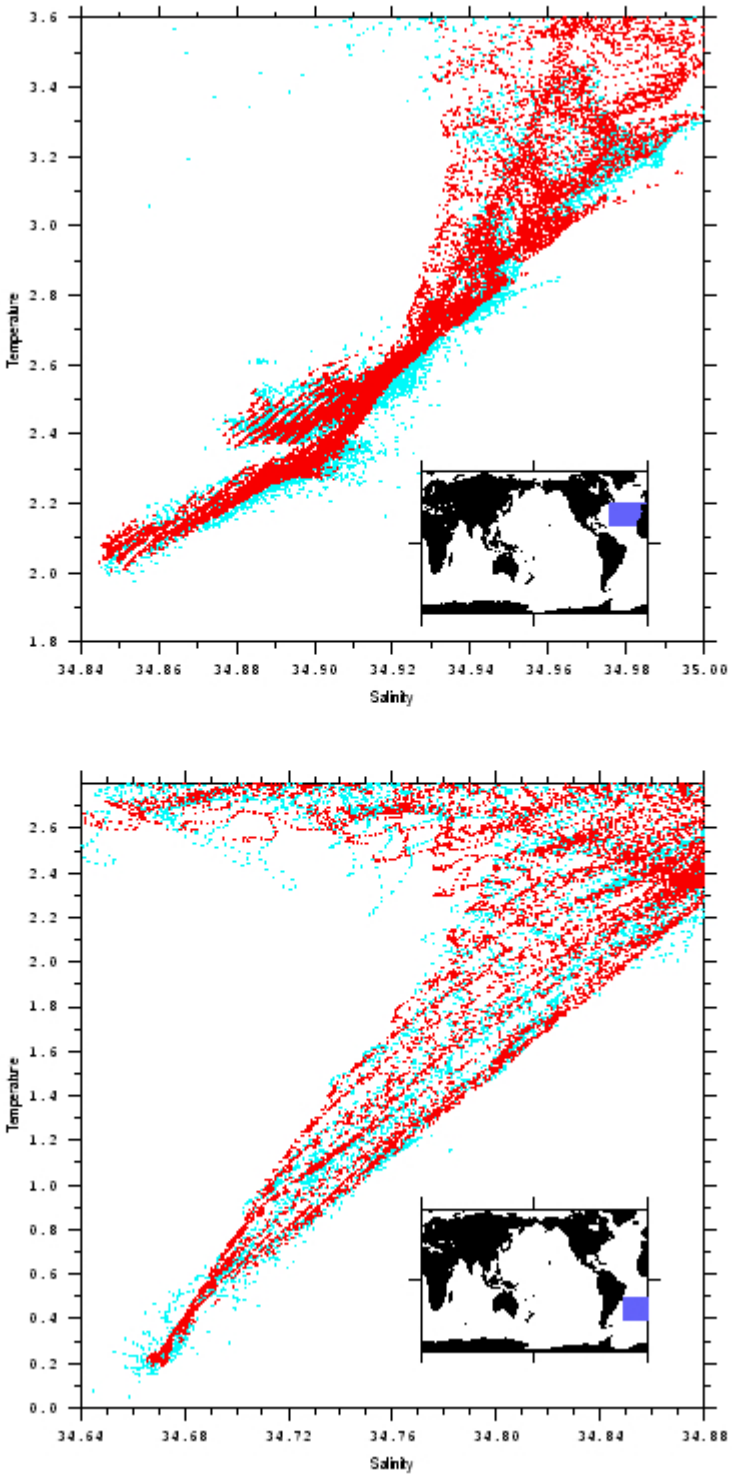

Fig. 15: Comparison between WGHC (red) and WOA01 (blue) climatologies for selected areas.

Another possible source of differences is the choice of the spatial interpolation procedure. The WOA01 climatology is constructed by using an interpolation method called successive correction (Cressman, 1959). There are indications that this method yields less consistent results (Sterl, 2001).

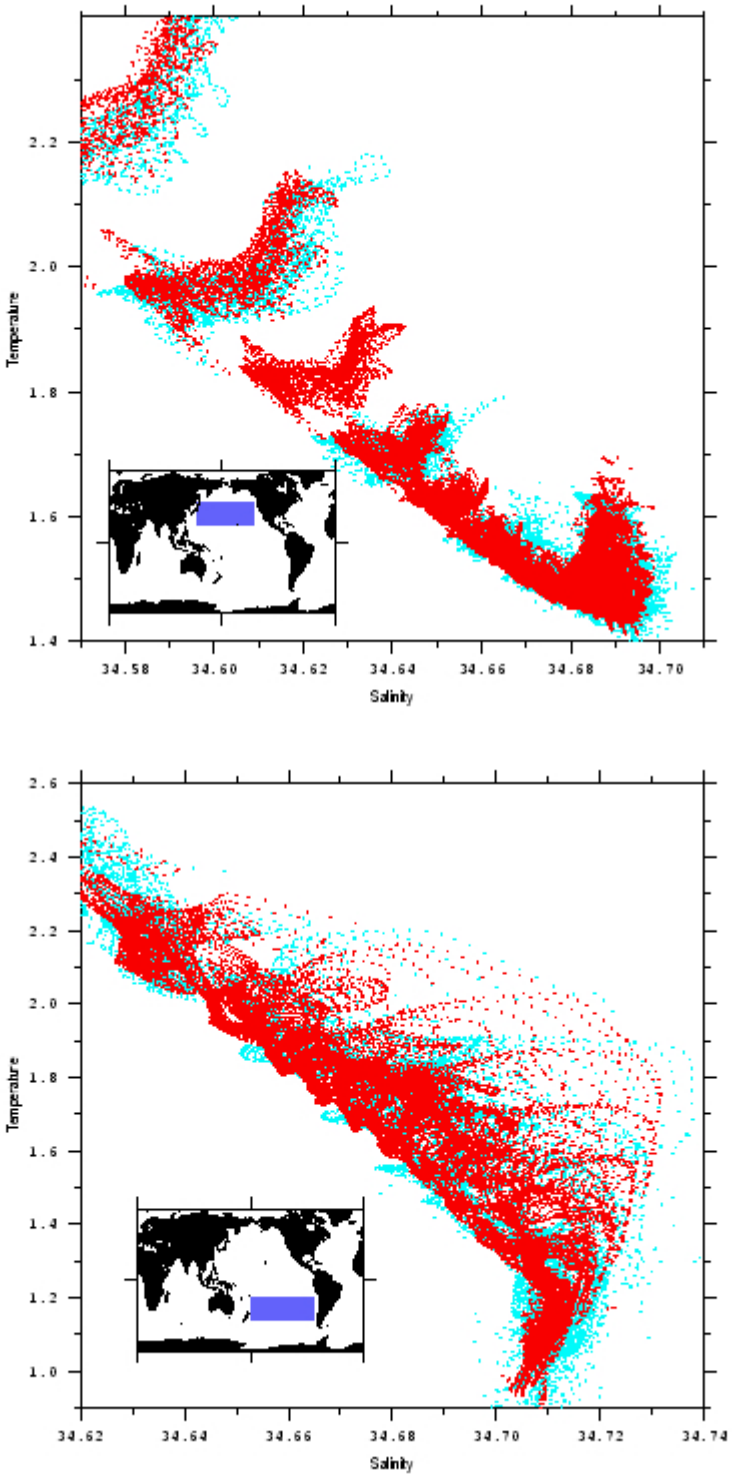

Fig. 15: (continued).

Significant differences also arise due to the way how the original data are averaged. We use averaging on isopycnal surfaces, whereas in the WOA01 climatology data are averaged on isobaric surfaces.

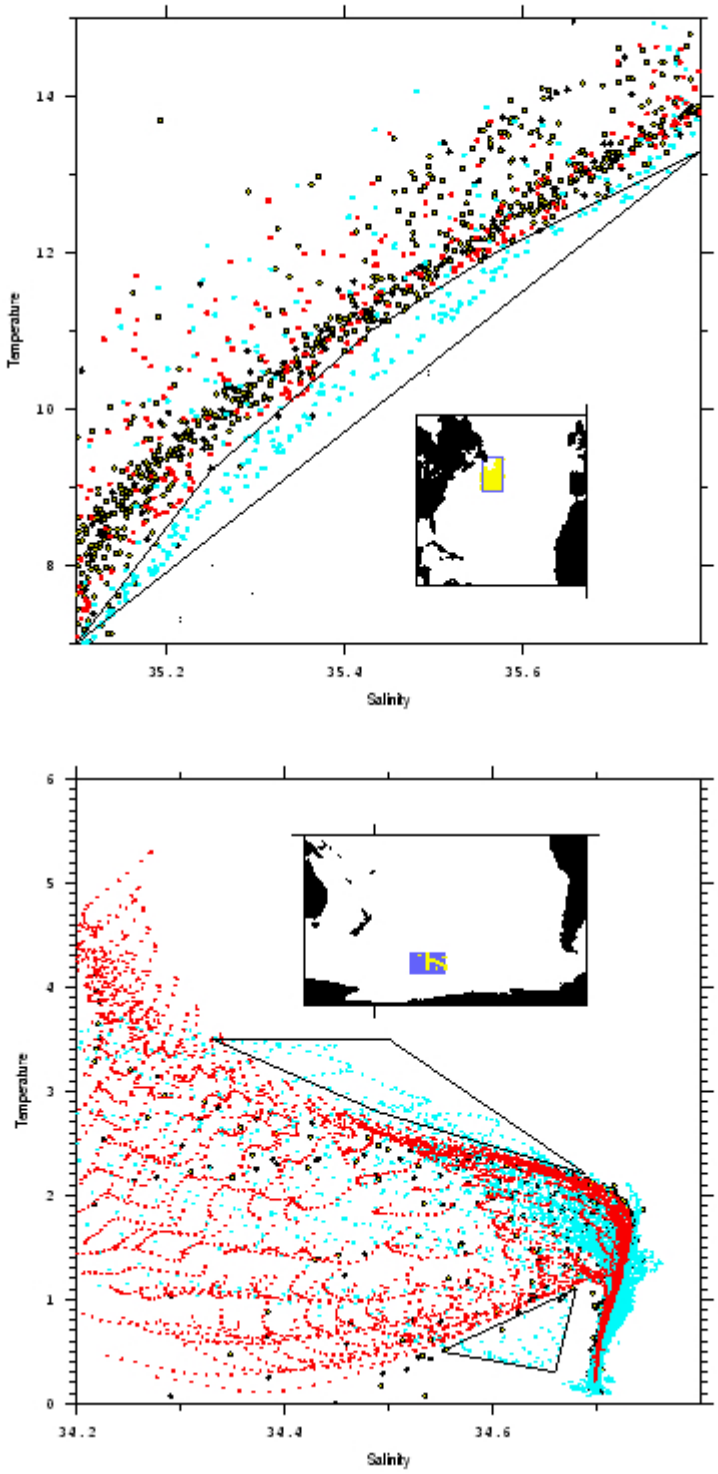

Fig. 16: Examples of artificial water mass production due to isobaric averaging in the WOA01 climatology. Black lines outline artificial water masses due to isobaric averaging of the data in the WOA01 climatology.

5.1. Differences in water mass characteristics

Potential temperature-parameter diagrams provide a good tool to document differences in water mass characteristics in both climatologies (**Fig.15**) . Lozier et al. (1994) were first to demonstrate the production of artificial water masses in the first World Ocean climatology by S.Levitus (1982) if averaging of the observed data is performed on isobaric surfaces. They also recommended to use an isopycnal averaging of the data in order to retain the observed thermohaline structure in the gridded (averaged) data. Gouretski and Jancke (1999) compared observed high quality hydrographic data in the South Pacific both with the WOA94 climatology and with their isopycnically averaged climatology. They found that WOA94 climatology produces artificial water masses within the central Ross gyre and along the Antarctic Circumpolar Current because of using an isobaric averaging of the data. It was also found, that the WOA94 climatology does not reproduce characteristic high-salinity shelf waters in the Pacific sector of the Southern Ocean.

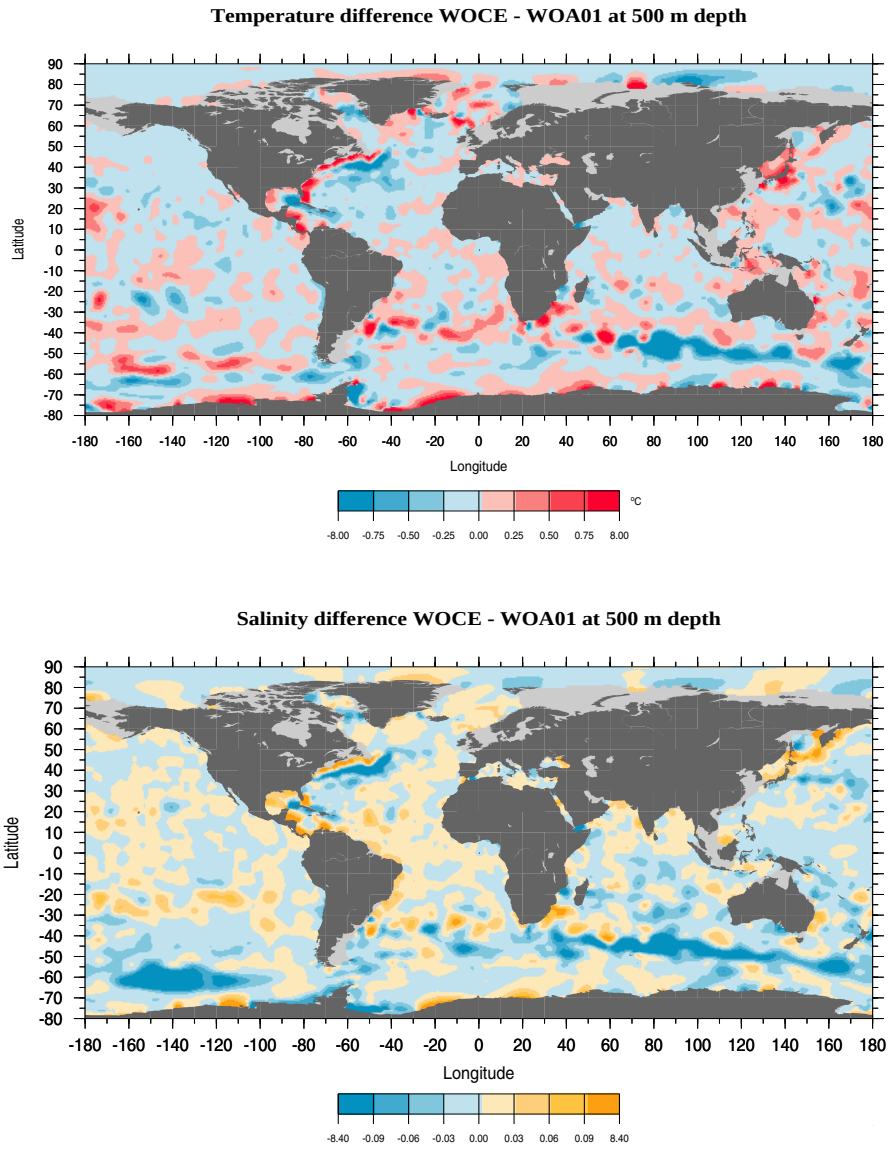

Fig. 17a: Temperature and salinity differences (WGHC-WOA01) for the 500 m depth level.

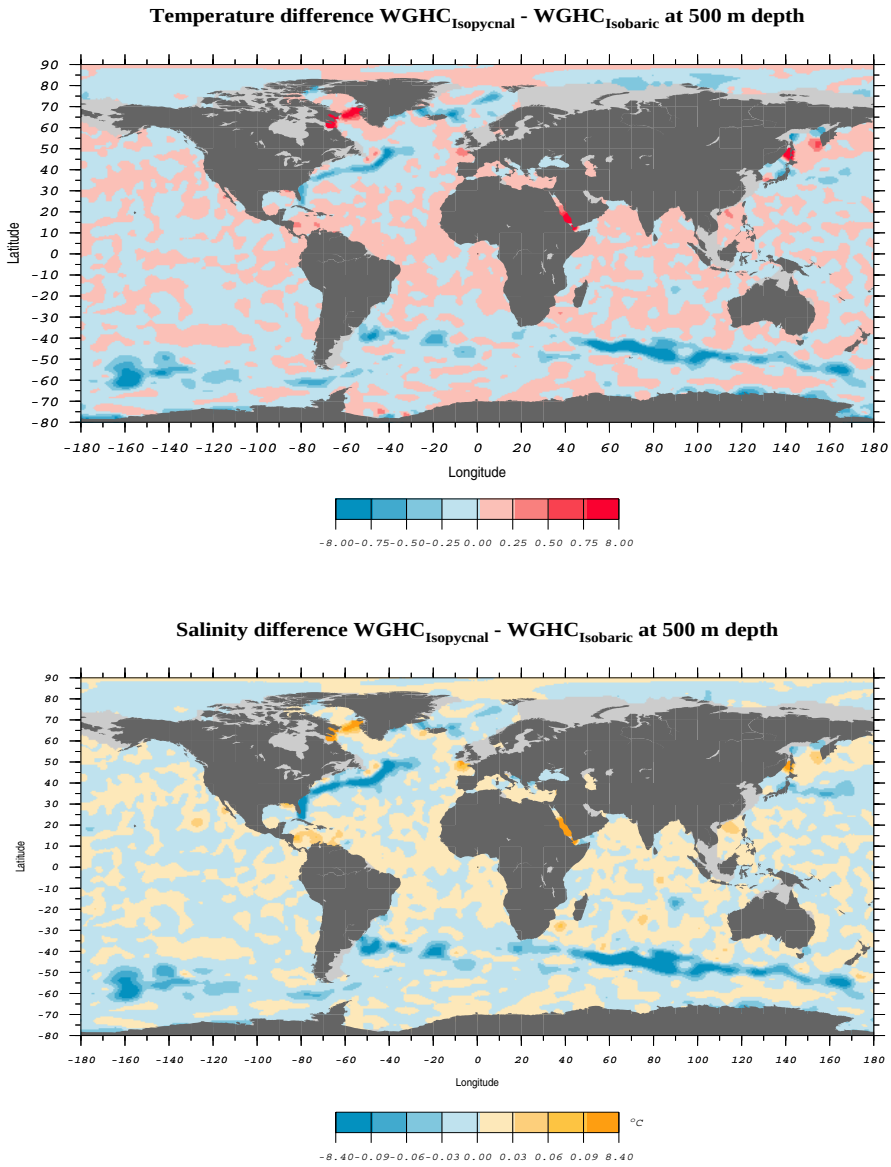

Fig. 17b: Temperature and salinity differences for the depth 500 m between isopycnally and isobarically optimally interpolated data.

Comparisons of our and the WOA01 climatology in θ-S space are presented in **Fig. 15** for selected regions of the World Ocean for data below 2000 m (North Atlantic, South Atlantic, South Pacific, North Pacific). Along with gridded data the observed data from the high-quality dataset are shown. Following differences are worth to note:

1) The WGHC climatology demonstrates tighter θ-S sequences compared with the WOA01 climatology, in a better agreement with high-quality data.
2) The WOA01 climatology tends to "overestimate" salinity for the same potential temperature compared with observed data and the WGHC climatology. Thus, in the South Pacific Ocean the WOA01 salinity is about 0.005 higher compared with original data.

Comparisons of the climatologies in θ-S space for two transects: across the Gulf Stream and across the Antarctic Circumpolar Current are presented in **Fig. 16.** Both regions are characterised by strong lateral property gradients, where isobaric/isopycnal averaging effects are supposed to be especially pronounced. Indeed, our comparison reveals artificial water masses in the WOA01 climatology. In the Gulf-Stream area within the potential temperature range 6-15 degrees an artificial water mass is observed with salinities up to 0.1 greater, compared with observations. In the ACC region the WOA01 climatology is also characterised by an anomalous water mass between ~2.5 and 6 ^{o}C, with salinity exceeding observed values by 0.05-0.1.

An overview of these effects is given in **Fig. 17**, where temperature and salinity differences between the WOA01 and WGHC climatologies are shown for the level 500 meters. A number of pronounced geographical patterns are observed, with the largest anomalies coinciding with such current systems, like Gulf-Stream, Kuroshio, Agulhas, and the ACC. It should be kept in mind, however, that the WOA01 input data are not identical to those used in our calculations. Therefore we repeated the calculations using the same optimal interpolation algorithm and the same input data but on isobaric surfaces. The result of the comparison allows to conclude, that most of the difference patterns of the **Fig.16** are really due to the effects of isobaric averaging of the data in WOA01 climatology.

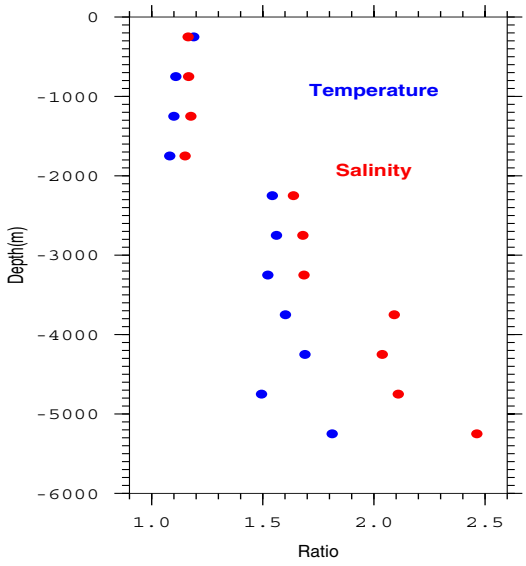

Fig. 18: Depth-bin-averaged absolute deviation of WOA01 and WGHC climatologies from the high-quality reference profile dataset. Ratio is defined as $|(f_{obs}-f_{WOA01})|/|(f_{obs}-f_{WGHC})|$.

A comparison was done between the global reference (observed) data set and both climatologies. Ratios of absolute differences $|(T_{obs}-T_{WOA01})|/|(T_{obs}-T_{WGHC})|$ and $|(S_{obs}-S_{WOA01})|/|(S_{obs}-S_{WGHC})|$ were computed for each observed T,S-pair. All depth-bin averaged ratios are greater than unit (**Fig. 18)**, indicating the WGHC climatology being closer to the high-quality data compared with the WOA01 climatology. The largest differences are observed in the deep water below 2000 m, where both temperature and salinity ratios exceed 1.5. Ratios of absolute deviations from observations averaged within 1x1 degree boxes and within the layer 250-500 meters are shown in **Fig.19** and demonstrate a generally much better agreement between the original observations and optimally interpolated fields for the WGHC climatology.

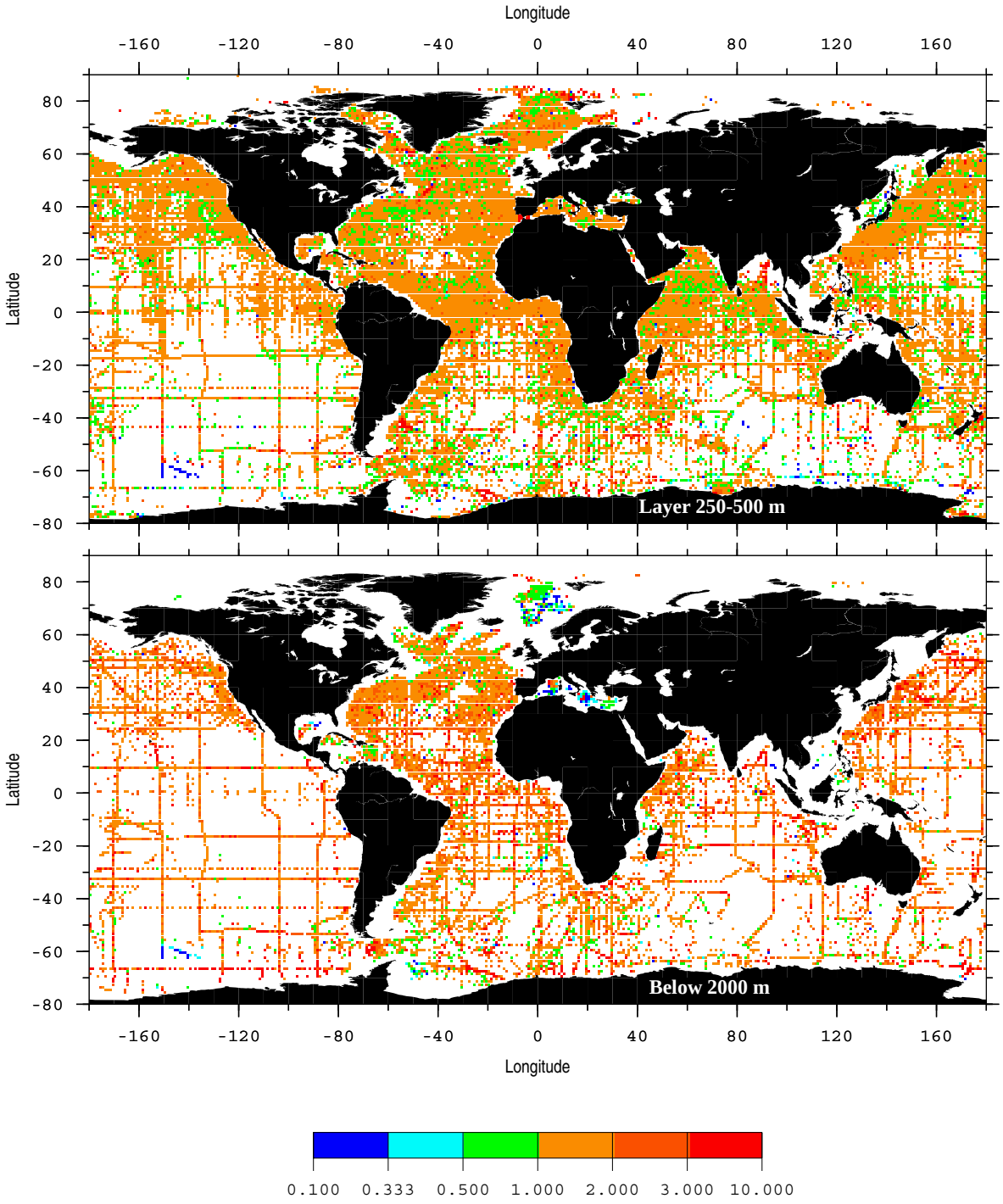

Fig.19: Relative fit of WOA01 and WGHC annual mean salinities to the observed high-quality data in 200-500 meter layer and below 2000m . Values greater than 1 indicate a better fit for the WGHC climatology.

An important improvement in the WGHC climatology is achieved through a finer vertical resolution. Whereas the WOA01 climatology has a relatively large spacing of 500 meters between the standard levels below 2000 m, the maximum vertical spacing in our climatology is 250 meters. The last level of the WGHC climatology is typically >=100 meters closer to

the actual (ETOPO5) bottom depth compared with the last WOA01 level (**Fig. 20**). In such deep regions as the North Pacific, Southwest Atlantic and Eastern Indian Ocean the last level of the WOA01 climatology is more than 250 meters above the bottom since the deepest gridded level is at 5500 meters.

5.2 Comparison of derived quantities

A comparison of steric height anomaly fields (**Fig.21)** reveals a high degree of similarity between the two climatologies. The shape and geographical location of many of circulation patterns (e.g. subtropical gyres, equatorial currents, Gulfstream and Kuroshio, Antarctic Circumpolar Current) are visually almost identical. The main difference is a considerably higher contrast between the regions of high and low steric height anomaly values. Thus, for the layer 50-1000 meters the steric height anomaly difference between the Ross Sea and the centre of the subtropical gyre is a factor of 1.3 higher for the WGHC climatology (130 cm comared with 100 cm for WOA01). The WGHC climatology better resolves such western boundary currents as the Gulfstream, Kuroshio, Agulhas. The ACC also appears as a more concentrated, narrower current in the WGHC climatology. The differences in terms of volume transports are better seen on individual sections. We present geostrophic volume transports between the grid points calculated relative to the deepest common level and accumulated transports for a 35.5^{o}N section across the North Atlantic and for the section along 20.5°E across the ACC (**Fig. 22)**.

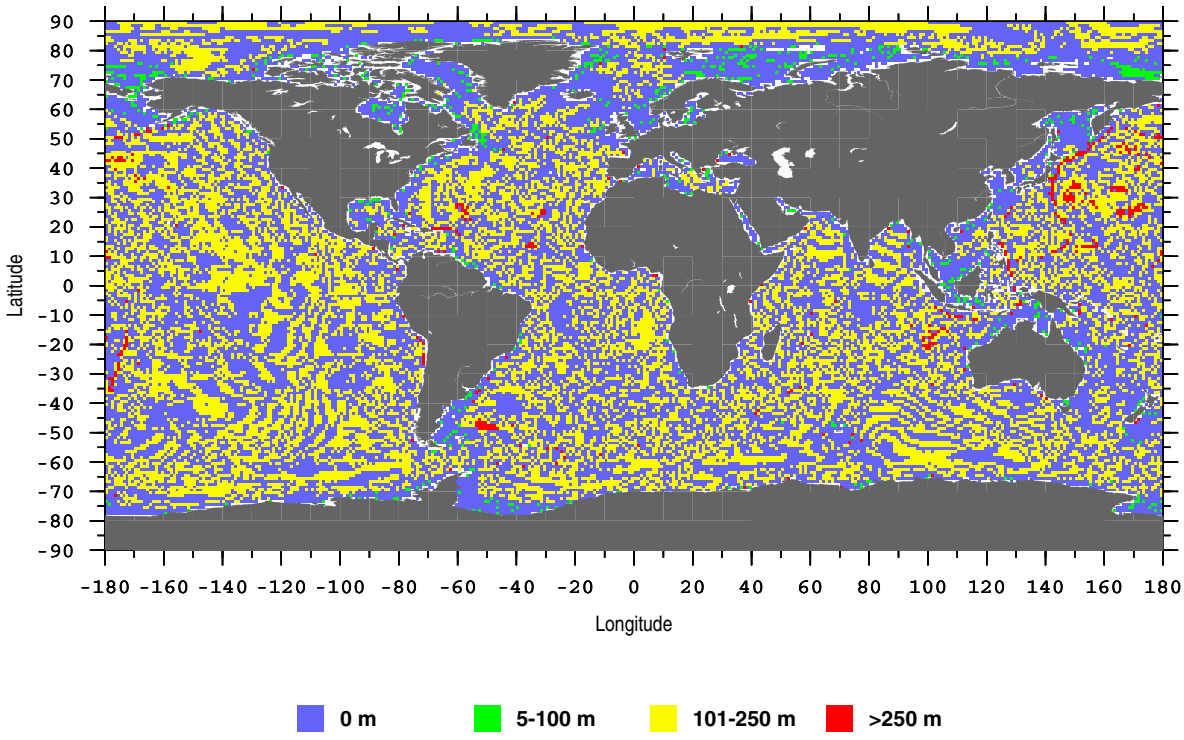

Fig.20: Difference (WGHC-WOA01) between the depths of the last gridded level.

5.3 Static stability of the gridded data

Hydrostatic instability of the gridded profiles poses a problem for a number of oceanographic applications. Thus, Jacket and McDougall (1995) had to artificially "stabilise" the WOA94 gridded data set in order to make it suitable for labelling observed hydrographic profiles with the neutral density γ^n variable. A test for hydrostatic stability was performed on the composite data-set used in this study. For the validated historical data 5% of the bottle pairs were found to be unstable, whereas for the original (not-validated) WOCE data the percentage was only 1%, indicating that inversions are mostly due to measurement errors and should not be considered real. Jacket and McDougall (1995) report instabilities of the gridded WOA94 climatology (see their Fig. 1a, page 382) and note that the problem areas are largely the Southern and Arctic Oceans, although all oceans are affected to some degree. We checked the latest WOA01 gridded climatology for hydrostatic instability and found, that the problem still remains (**Fig. 23**).

Instabilities occur at about half of all grid points, with gridded profiles exhibiting more unstable standard level pairs in the Polar Ocean, Southern Ocean, Mediterranean Sea, Okhotsk Sea and some other regions. The vertical distribution of unstable level pairs and of the number of inversions is given in **Fig. 24**.

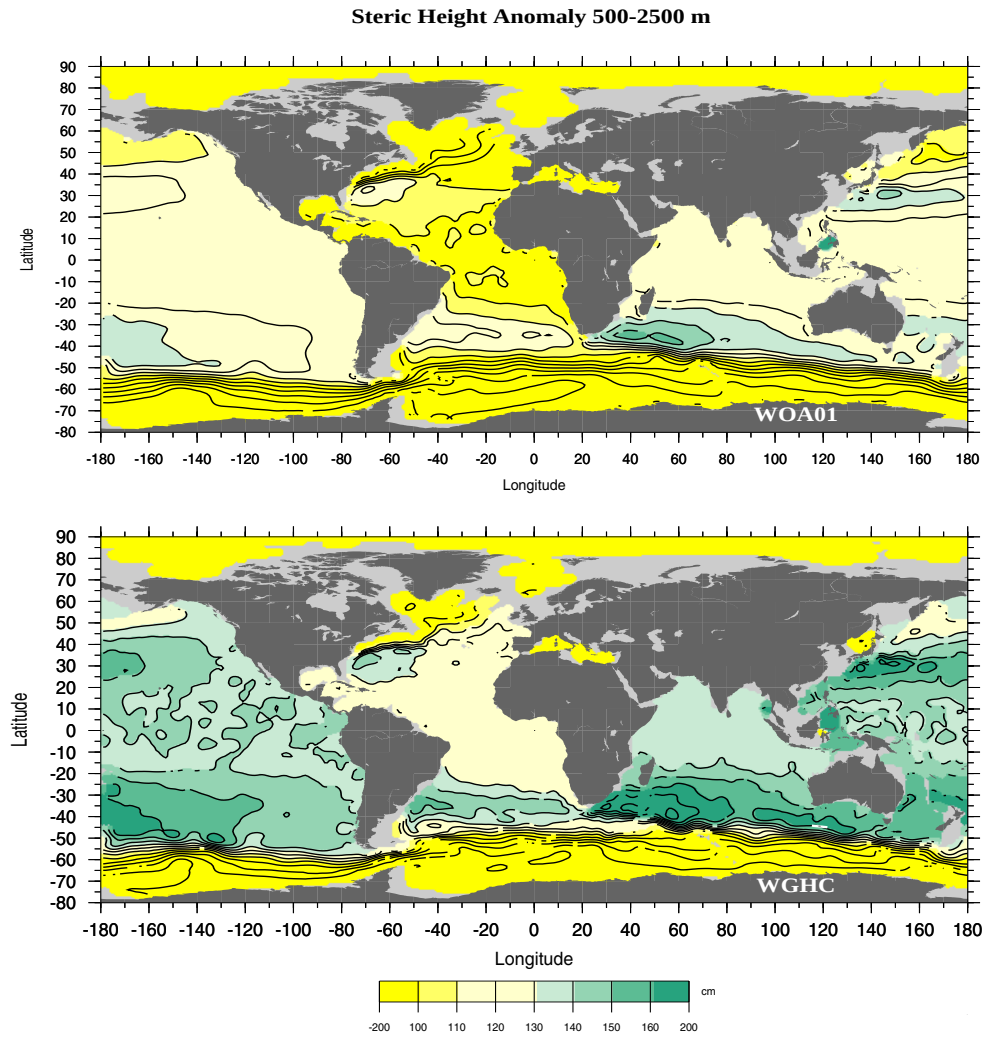

Fig. 21: Steric height anomaly for the layer 500-2500 m.

The stabilisation of the gridded profiles in the WGHC climatology was done assuming that it is mostly errors in salinity which are responsible for the instability. For each unstable pair of gridded levels, salinities of upper/lower levels were decreased/increased iteratively until the stability of the pair was achieved (an increment of 0.00001 PSS was used). The procedure starts with the uppermost unstable pair and is repeated until the stability of the whole profile is achieved. The procedure thus "spreads" the salinity error in the vertical reducing individual salinity corrections. We note that typical corrections are small (an order of 10^{-4}).

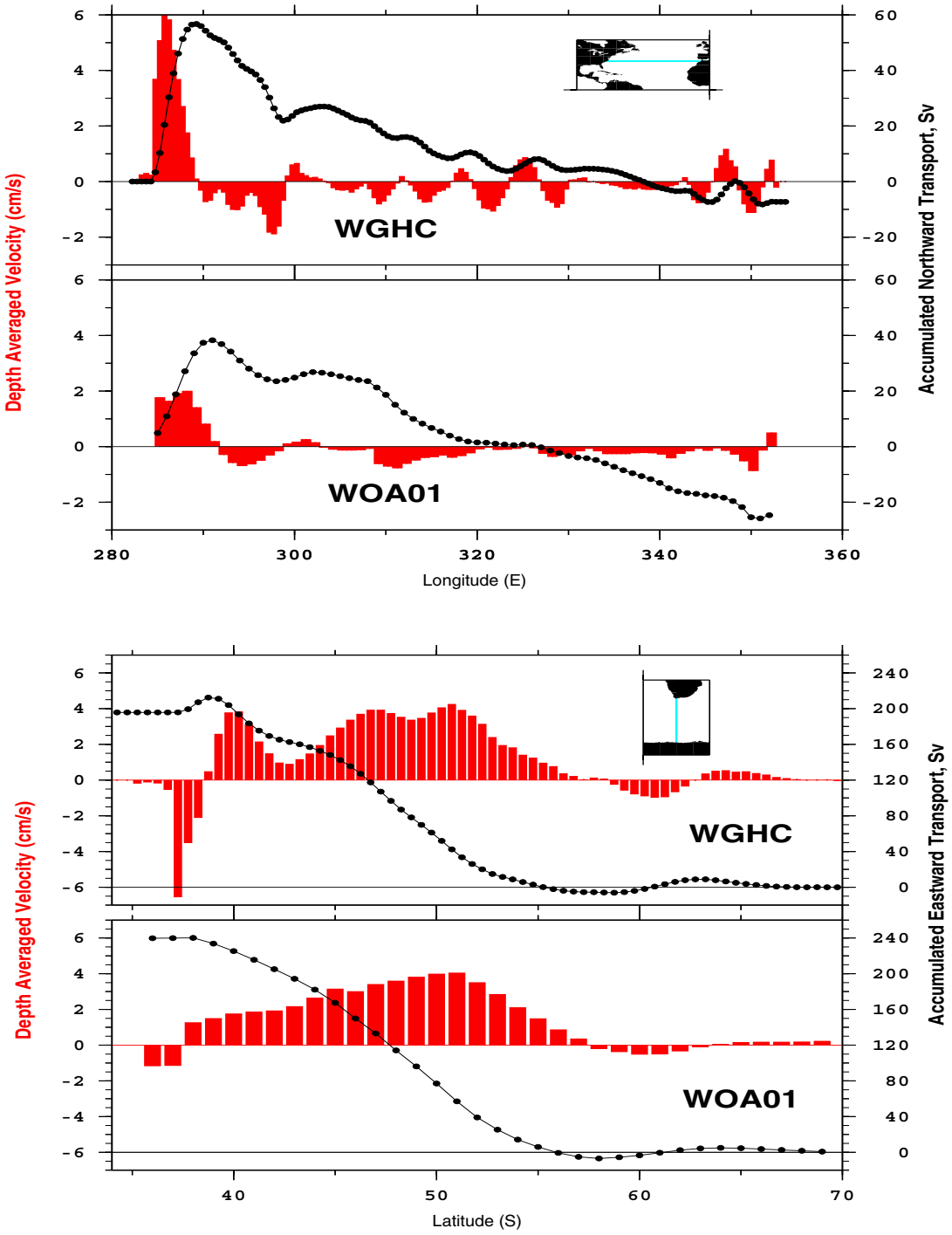

Fig. 22: Bottom to surface geostrophic transports (black) and depth-averaged velocities (red bars) for the zonal section along 34.5°N (two upper panels) and for the meridional section along 20.5°E (two lower panels) as calculated on the basis of WOA01 and WGHC climatologies.

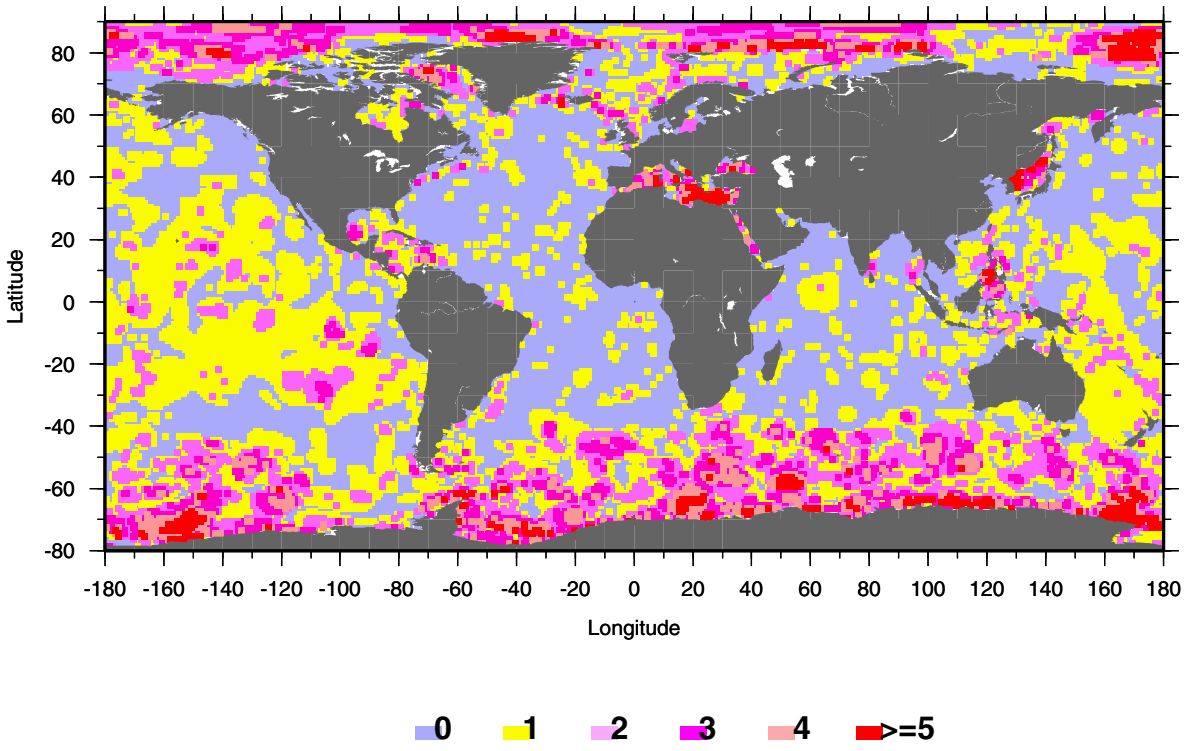

Fig. 23 : Number of unstable standard level pairs per gridded profile in WOA01 climatology. Only density inversions corresponding to the density difference of > 0.001 kg/m^3 between two gridded levels are considered.

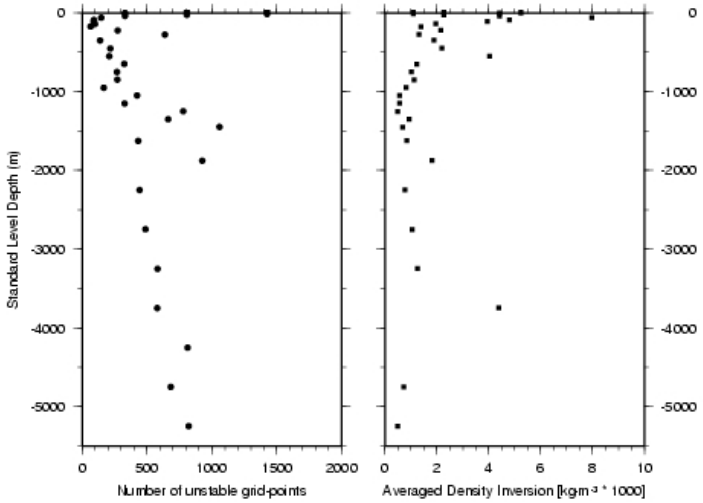

Fig. 24. Average number of unstable standard level pairs (a) and average density inversion vs depth in WOA01 climatology.

6. Caspian Sea Climatology

A dataset obtained from the Institute of Geography, Baku, Azerbajdjan, allowed us for the first time to calculate a climatology for the Kaspian Sea, the Earth´s largest interior sea. Climatological distributions of temperature and salinity were calculated on the same 0.5x0.5 degree grid with the same vertical resolution as for the Global Ocean. Here we provide only two examples of property distributions at selected standard levels **(Fig. 25).** Bottom relief is provided by the Caspian Environment Program (2002).

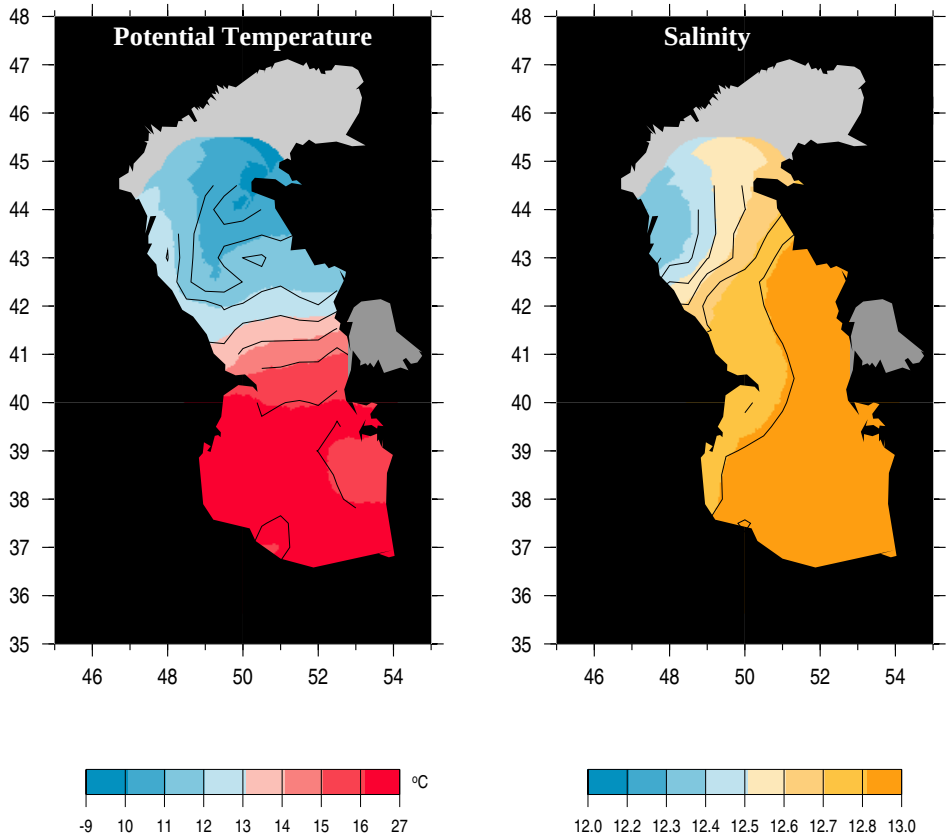

Fig. 25: Annual mean distribution of potential temperature and salinity at 10 meter depth in the Caspian Sea.

7. Integral characteristics of the gridded dataset

The annual gridded climatology was used to obtain some integral property characteristics of the World Ocean. Gridded properties were averaged with weighting accounting for the respective area and depth range as represented by each grid-node. Volume-averaged values were obtained for the Global Ocean and for the Polar, Atlantic, Indian, Pacific, and Southern oceans separately as shown in **Fig. 26**. Hudson Bay, Baltic Sea, Black Sea, Mediterranean Sea are included into the Atlantic domain, Red Sea and the Persian Gulf are included into the Indian Ocean domain, and seas of the Indonesian Archipelago belong to the Pacific domain. The latitude 30^{o}S is assumed as the northern boundary of the Southern Ocean.

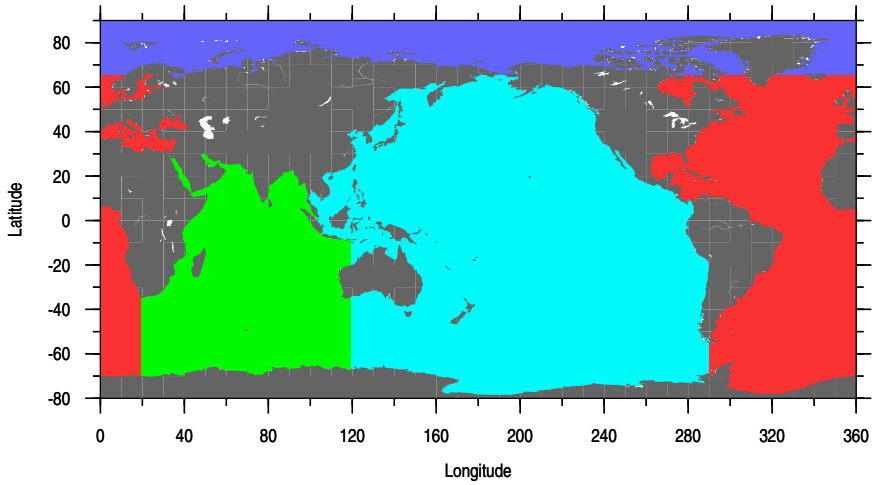

Fig.26. Main ocean basins for which volume-averaged parameters have been calculated (see Table 1)

Table 1. Volume-averaged parameters for the main World Oceans as based on the gridded WOCE Hydrographic Climatology *)

OCEAN	T (°C)	Θ (°C)	Salinity	Oxygen (ml/l)	Silicate (μmol/kg)	Nitrate (μmol/kg)	Phosphate (μmol/kg)	Sigma-0 (kg/m^3)	Area (km^2)	Volume (km^3)
GLOBAL	3.8142 *5574382*	3.6460 *5574382*	34.7229 *5569065*	3.9199 *5571225*	88.1835 *5564439*	31.2087 *5563021*	2.1670 *5562954*	27.4865 *5564798*	360808032 *171071*	1298060310 *5574382*
POLAR	-0.1945 *618393*	-0.2642 *618393*	34.7139 *617961*	6.9427 *617857*	9.7787 *617048*	13.1146 *617610*	0.9546 *617672*	27.8805 *618405*	13340939 *25647*	16630286 *618393*
ATLANTIC	4.2636 *1309580*	4.0882 *1309580*	34.9352 *1305908*	5.1149 *1307049*	44.3891 *1306020*	22.8536 *1303442*	1.5842 *1303308*	27.6002 *1298226*	92846458 *40626*	322453728 *1309580*
INDIAN	3.9864 *969300*	3.8270 *969300*	34.7552 *968087*	4.0027 *967187*	88.9434 *967062*	31.7037 *966744*	2.2233 *966751*	27.4795 *968333*	68163250 *27936*	247991233 *969300*
PACIFIC	3.6437 *2677109*	3.4733 *2677109*	34.6154 *2677109*	3.2781 *2679132*	109.6173 *2674309*	35.2450 *2675225*	2.4398 *2675223*	27.4283 *2679834*	186457385 *76839*	710985063 *2677109*
SOUTHERN	2.5894 *2003778*	2.4363 *2003778*	34.6382 *2003778*	4.7451 *2050272*	84.3408 *2001718*	30.7932 *2000858*	2.1298 *2000721*	27.5913 *1992319*	10796981 *57823*	403406857 *2003778*

*) Number of affected grid-nodes is given in italics. Areas are calculated assuming spherical Earth with the radius of 6371 km. ETOPO5 bathymetry is used for the calculations of areas and volumes. Also note that throughout this report the SI definitions for salinity are adhered to (Siedler, 1998)

Volume T,S-diagrams were computed for the Global Ocean based on the gridded climatological fields. **Fig. 27** gives an example of such diagram for the temperature range -2 to 4 °C and for the salinity range 34.5 to 35, which comprise the most voluminous water masses.

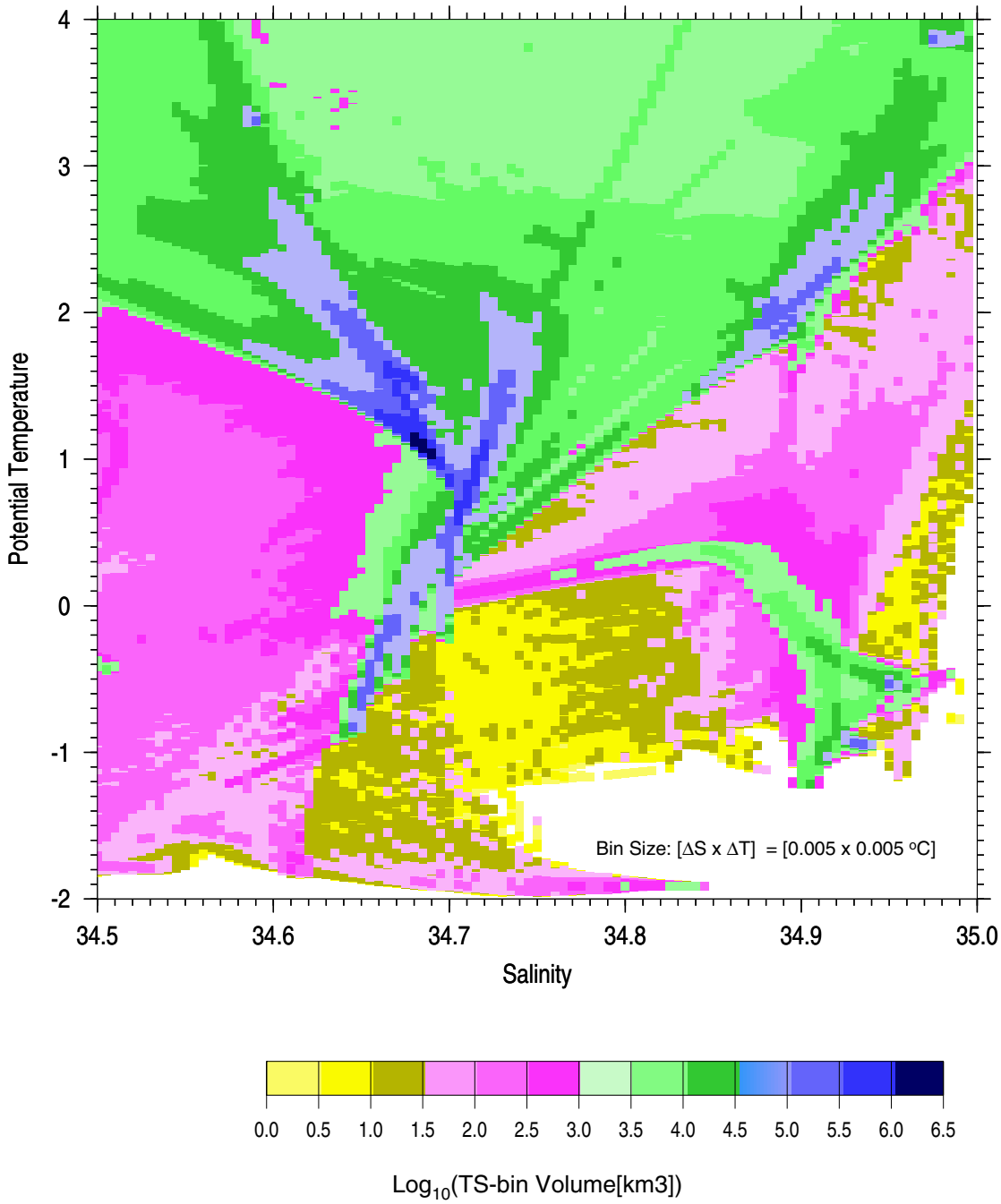

Fig. 27: Volume T,S-diagram for the World Ocean based on the WGHC climatology.

8. Error estimates for the observed and gridded data

8.1. Observed data

WOCE hydrographic data comprise the main part of the reference dataset used in this study. For the first time a uniformly accurate dataset was obtained for the Global Ocean, with the quality standards for water samples set by the WOCE Hydrographic Program (WOCE Operations Manual, 1991). An objective method was applied to the almost complete set of WOCE hydrographic cruises to calculate inter-cruise offsets (Gouretski and Jancke, 2001). It was shown, that quality requirements for the WOCE Hydrographic Programme have been obviously fulfilled (Table 2).

Table 2. WHP one-time survey standards for water samples

Property	**WOCE standard (accuracy / precision) (from WHP Manual, 1994)**	**Average WOCE inter-cruise offset (Gouretski&Jancke, 2001)**
Temperature	0.005 / 0.002 ^{o}C	-
Salinity	0.002 / 0.001	0.0019
O_2	~1% / 0.1%	~1.4%
NO_3	~1% / 0.2%	~1.6%
PO_4	~1-2% / 0.4%	~1.9%
SiO_2	~1-3% / 0.2%	~2.6%

Accuracy of historical hydrographic data varies strongly between the cruises with possible errors being generally an order of magnitude higher compared with the reference data.

8.2. Gridded data

A formal squared absolute objective interpolation error is :

$$\varepsilon^2 = \sigma^2 \varepsilon'^2 ,$$

where σ^2 is a property variance and ε' is the relative error of the objective interpolation. Absolute formal errors are largest in the upper layers, where property variability is strong, and decrease rapidly with depth as shown in the **Fig. 27**. We note that the error estimate is inaccurate, because the "true" covariance function is unknown (a useful discussion is given by Sokolov and Rintoul, 1999)

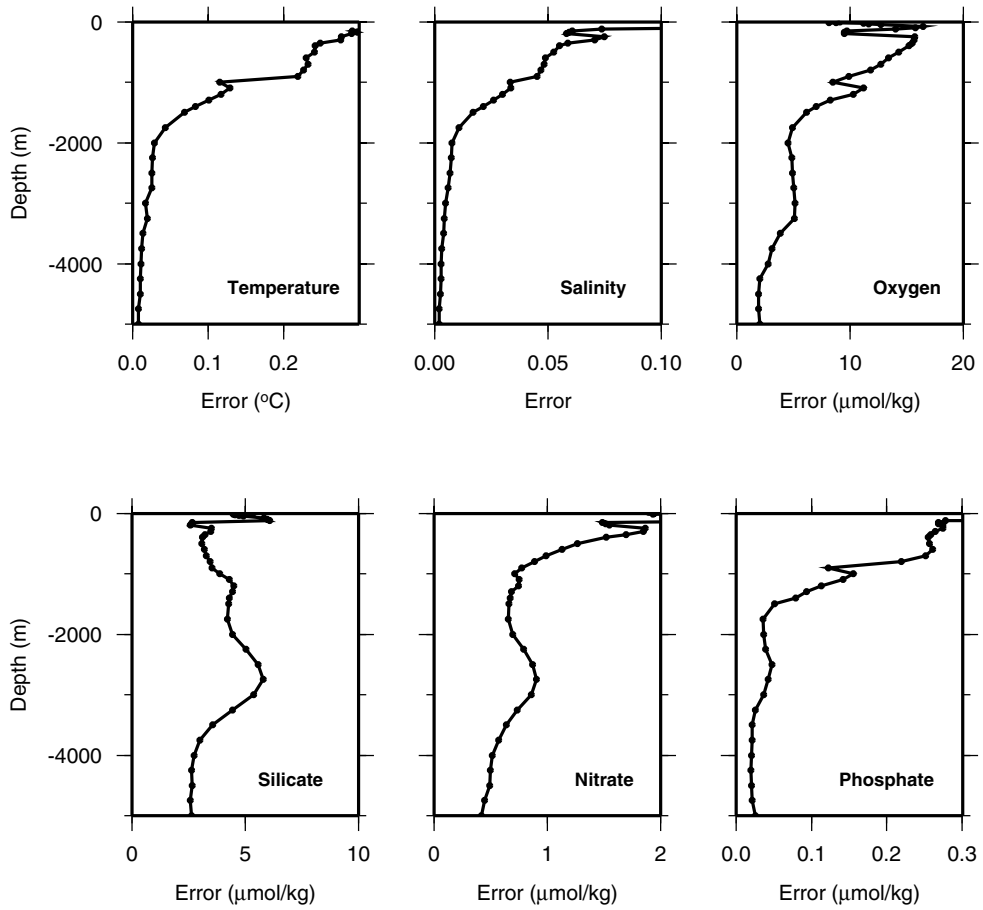

Fig. 27: Area averaged formal error of the optimal interpolation vs depth

9. CD-ROM contents

The WGHC climatology is available on two CD-ROM disks provided along with this report and containing observed and gridded data respectively. Further information is available under http://www.bsh.de. The climatology and the WOCE Atlantic Atlas site are available under: http://www.bsh.de/de/Meeresdaten/Beobachtungen/Klima/WOCE-AIMS/index.jsp

9.1. CD-ROM-1: Observed data

This report is contained on the CD-ROM-1 as a pdf-file. This CD-ROM also contains observed profile data used in the production of this climatology. There are 169 data files, each file including profiles from a 1-degree-latitude zone:

File	Northern Boundary	Southern Boundary
001_wghcob	90°N	89°N
002_wghcob	89°N	88°N

.....	.....	.....
169_wghcob	78°S	79°S

A FORTRAN program ***read_observed_data.f*** is an example program which reads in profiles in the selected data file and prints them to screen.

SAMPLE OBSERVED PROFILE

```
A  100115009 JAMES CLARK ROSS              UNITED KINGDOM  A23_JC10/1      WOCE_IPO
B     100115          9  1 ROS OBS         0
C 1995  3 31  8  6 BO  -71.9557  -18.2188 GP
D    14 2990.8 3043.6 2990.8    7.9 3058.0 P 13  1 OBSERV
E    -9.0   -9.0 -9.0000 -9.0000  0.0012 -9.0000 -9.0000 -9.0000 -9.0000  1.029   1.00  0.981  1.015
    7.8    7.9 -1.7971 -1.7972 34.1940 27.5256 36.9594 45.9681 27.7736 -9.900  66.47 27.870  1.850 00000000 00000000 00000000
   52.4   53.0 -1.7883 -1.7893 34.1973 27.5282 36.9614 45.9696 27.7772  7.629  66.29 27.820  1.830 00000000 00600000 00000000
  154.1  155.8 -0.4367 -0.4418 34.5337 27.7517 37.0964 46.0216 28.0391  5.505  84.41 32.010  2.140 00000000 00000000 00000000
  203.9  206.2  0.3670  0.3588 34.6187 27.7786 37.0747 45.9540 28.0779  5.010  90.72 32.600  2.170 00000000 00000000 00000000
  254.0  256.9  0.6625  0.6514 34.6549 27.7903 37.0690 45.9316 28.0970  4.759  94.13 32.100  2.170 00000000 00000000 00000000
  354.1  358.2  0.8696  0.8533 34.6873 27.8036 37.0701 45.9215 28.1214  4.672  98.44 32.310  2.160 00000000 00000000 00000000
  506.3  512.3  0.7820  0.7582 34.6963 27.8170 37.0889 45.9452 28.1549  4.601 101.96 32.020  2.150 00000000 00000000 00000000
 1008.0 1021.2  0.4050  0.3563 34.6832 27.8308 37.1261 46.0044 28.2063  4.766 113.22 32.510  2.180 00000000 00000000 00000000
 1259.3 1276.5  0.2484  0.1863 34.6771 27.8354 37.1406 46.0284 28.2303  4.808 116.92 32.630  2.190 00000000 00000000 00000000
 1513.6 1535.1  0.1344  0.0577 34.6728 27.8390 37.1519 46.0469 28.2523  4.941 116.45 32.760  2.190 00000000 00000000 00000000
 1766.8 1793.0  0.0451 -0.0472 34.6702 27.8424 37.1616 46.0624 28.2745  5.052 117.67 32.500  2.190 00000000 00000000 00000000
 2017.9 2049.0 -0.0306 -0.1392 34.6681 27.8456 37.1700 46.0760 28.2936  5.114 118.09 32.530  2.180 00000000 00000000 00000000
 2516.6 2558.2 -0.1333 -0.2778 34.6639 27.8491 37.1819 46.0957 28.3218  5.245 117.95 32.230  2.170 00000000 00000000 00000000
 2990.8 3043.6 -0.1780 -0.3609 34.6618 27.8514 37.1892 46.1078 28.3391  5.411 118.33 32.090  2.160 00000000 00000000 00000000
/T=0.and S=35. were used to convert dbars into meters
```

9.2. CD-ROM-2: Gridded data

The CD-ROM-2 contains objectively analysed all-data-mean profiles for one-half-degree squares for the Global Ocean. We use 45 standard depth levels extending from the sea surface to 6000 meter depth. The data are split into 6 files, each file representing a 59.5-degree longitude sector of the World ocean.

Filename	Longitude, E
Wghc_0000-0595.gz	0- 59.5
Wghc_0060-1195.gz	60-119.5
Wghc_1200-1795.gz	120-179.5
Wghc_1800-2395.gz	180-239.5
Wghc_2400-2995.gz	240-299.5
Wghc_3000-3595.gz	300-359.5

The header of each gridded profile contains the number of gridded levels, radius of influence bubble, decorrelation length scale and mixed layer depth. Each standard level contains analysed values of temperature, salinity, oxygen, silicate, nitrate, and phosphate, along with relative interpolation errors, number of observations contributed to the optimum estimate, and property standard deviations within the influence bubble.

The first grid-node in the first file (wghc_0000-0595.gz) represents the 0.5x0.5-degree box centred at 80°S and 0°. The first 341 grid-nodes are incremented northward constant in longitude. The 342-th grid-node has the coordinates 80°S and 0.5°E. Each of the six files follows the same pattern with the longitude of the first grid node being incremented by 60 degree in longitude.

The sample FORTRAN program ***read_wghc_climatology.f*** reads in gridded profiles. The program requests a single latitude and longitude of the grid node from the user and returns gridded properties at standard levels written to the screen. The user should modify the program according to specific needs.

SAMPLE GRIDDED PROFILE

```
17  900.  444.  91.
  0.0 -42.0  505.    0.    0. 10.683307 10.683308 34.425133   6.364    2.82   6.747   0.877 0.03 0.04 0.09 0.36 0.32 148 100  57  31  57   2.989
0.382  0.554  1.847  6.415  3.984 26.444109 26.384766 35.174927 43.579956
  0.0 -42.0  505.   10.   10. 10.744557 10.743351 34.439049   6.367    2.54   6.791   0.879 0.02 0.04 0.09 0.36 0.32 160 100  59  29  55   3.031
0.383  0.536  1.769  6.260  3.969 26.444214 26.385010 35.172607 43.574951
  0.0 -42.0  505.   20.   20. 10.639179 10.636784 34.422794   6.391    2.09   7.469   0.856 0.02 0.03 0.07 0.16 0.27 160 100  78  43  72   3.096
0.378  0.536  2.120  6.553  3.942 26.450829 26.391357 35.183472 43.590210
  0.0 -42.0  505.   30.   30. 10.635305 10.631711 34.421646   6.324    2.01   8.218   0.863 0.02 0.08 0.24 0.30 0.26 160  97  60  51  80   3.079
0.375  0.556  2.523  6.702  3.808 26.450802 26.391235 35.183594 43.590576
  0.0 -42.0  505.   40.   40. 10.628573 10.623780 34.423038   6.319    2.16   8.403   0.880 0.02 0.07 0.23 0.30 0.26 160  98  61  52  84   2.983
0.373  0.554  2.461  6.711  3.834 26.453365 26.393677 35.186401 43.593628
  0.0 -42.0  505.   50.   50. 10.466343 10.460410 34.420265   6.310    2.19   8.890   0.891 0.02 0.08 0.23 0.29 0.26 160 100  63  55  96   3.075
0.389  0.564  2.727  6.843  3.836 26.481808 26.420288 35.219727 43.633423
  0.0 -42.0  505.   75.   76. 10.068050 10.059361 34.431335   6.230    2.35   8.716   0.916 0.02 0.08 0.22 0.30 0.26 160  92  61  39 103   3.016
0.407  0.591  2.862  6.543  3.696 26.565388 26.498169 35.314453 43.743774
  0.0 -42.0  505.  100.  101.  9.609494  9.598232 34.445004   6.208    2.44   9.975   0.957 0.02 0.05 0.08 0.23 0.26 160 100  83  51 106   3.055
0.403  0.597  3.098  6.360  3.722 26.660105 26.586548 35.422363 43.869629
  0.0 -42.0  505.  125.  126.  9.322761  9.308925 34.478439   6.189    2.94  11.469   1.000 0.03 0.04 0.06 0.20 0.25 144 100  99  64 120   1.203
0.260  0.582  3.726  6.575  0.922 26.740353 26.660156 35.507935 43.966675
  0.0 -42.0  505.  150.  151.  9.100936  9.084558 34.496937   6.154    3.26  12.553   1.043 0.03 0.03 0.05 0.12 0.25 144 100 100  77  94   1.057
0.225  0.525  1.385  1.799  0.831 26.796394 26.711060 35.568237 44.035767
  0.0 -42.0  505.  175.  176.  8.849586  8.830782 34.501427   6.110    3.71  13.662   1.101 0.03 0.03 0.05 0.10 0.24 128 100 100  83 100   0.907
0.191  0.519  1.426  1.671  0.751 26.845415 26.754883 35.623169 44.101196
  0.0 -42.0  505.  200.  202.  8.575100  8.553992 34.494553   6.075    4.28  14.769   1.151 0.03 0.03 0.04 0.10 0.24 128 100 100  86 104   0.801
0.165  0.510  1.531  1.503  0.809 26.888245 26.792847 35.673462 44.162842
  0.0 -42.0  505.  250.  252.  8.123867  8.098262 34.487511   5.922    5.50  17.029   1.262 0.04 0.05 0.09 0.44 0.25 112 146 128  86  92   0.682
0.131  0.550  1.418  1.160  0.886 26.960810 26.856812 35.757935 44.266602
  0.0 -42.0  505.  300.  303.  7.471601  7.442278 34.453213   5.728    7.10  19.687   1.403 0.04 0.05 0.08 0.44 0.25 112 151 132  92  98   0.703
0.123  0.597  1.904  1.008  0.930 27.040213 26.926025 35.857666 44.394775
  0.0 -42.0  505.  350.  353.  6.847847  6.815214 34.413425   5.615    8.49  22.143   1.539 0.04 0.05 0.10 0.44 0.29  96 140 140 102 105   0.814
0.131  0.586  2.029  0.753  0.806 27.105383 26.982178 35.943604 44.508545
  0.0 -42.0  505.  400.  404.  6.201556  6.166132 34.369289   5.596   10.17  23.967   1.657 0.04 0.06 0.11 0.46 0.30  96 140 140  97 102   0.817
0.124  0.557  2.087  0.660  0.650 27.165693 27.033203 36.026123 44.620850
  0.0 -42.0  505.  500.  505.  4.903539  4.863990 34.266869   5.666   13.44  26.017   1.794 0.05 0.07 0.12 0.41 0.33  96 120 120 110 111   0.582
0.083  0.483  2.174  0.588  0.055 27.260653 27.109619 36.167969 44.824097
```

Acknowledgements:

Our thanks go to many WOCE principal investigators who provided us with their hydrographic data. Discussions on the hydrostatic stability of the gridded data with Dr. D. Jackett were very helpful. Dr. R. Mamedov has generously provided Caspian Sea hydrographic data. V.V. Gouretski was supported through the grants 03F0378A and 03F0157B from the Bundesministerium für Bildung und Forschung.

References:

Bretherton, F.P., R.E. Davis, and C.B. Fandry (1976) A technique for objective analysis and design of oceanic experiments. *Deep-Sea Res*earch, 23, p.559-582.

Caspian Environment Programme (2002) http://www.caspianenvironment.org/

Cressman, G.P. (1959) An operational objective analysis scheme. *Monthly Weather Review*, 87, 329-340.

Conkright, M.E., S. Levitus, T.P. Boyer (1994) World Ocean Atlas 1994. Vol.1: Nutrients. NOAA Atlas NESDID 1, U.S.Gov. Printing Office, Washington D.C., 150 pp.

Conkright, M.E., J.I. Antonov, O.K. Baranova, T.P. Boyer, H.E. Garcia, R. Gelfeld, D.Johnson, R.A. Locarnini, P.P. Murphy, T.D. O'Brien, I. Smolyar, C. Stephens (2002) World Ocean Database 2001. Vol.1: Introduction. NOAA Atlas NESDID 42, U.S.Gov. Printing Office, Washington D.C., 159 pp.

Culberson, C.H., Knapp, G., Stalcup, M., Williams, R.T. and Zemlyak, F. (1991) A comparison of methods for the determination of dissolved oxygen in seawater. WHP Office Report 91-2, WOCE Report 73/91, WHOI, Mass., USA, 77 pp.

Curry, R.G. (1996) HydroBase: A Database of hydrographic stations and tools for climatological analysis. *WHOI Technical Rep*ort WHOI-96-01.-50 pp.

Curry, R. (2000) HydroBase2. In: *2000 U.S.WOCE Report*, p. 14-16).

Gandin, L.S. (1963) Objective analysis of the meteorological fields. Leningrad, Gidrometeoizdat, 287 pp. (in Russian) (English translation No.1373 by Israel Program for Scientific Translations (1965), Jerusalem, 242 pp.)

Gordon, A.L. and E.L. Molinelli (1982). *Southern Ocean Atlas*. Part I, Thermohaline and Chemical Distributions and Atlas Data Set, Columbia University Press, New York, 11 pp., 233 Plates.

Gouretski, V.V. and K. Jancke (1995) A consistent pre-WOCE hydrographic data set for the South Atlantic: station data and gridded fields. *WHP SAC Technical Report No.1*, WOCE Report No. 127/95, Hamburg, 32 pp. [unpublished manuscript].

Gouretski, V.V. and K. Jancke (1996) A new hydrographic data set for the South Pacific: synthesis of WOCE and historical data, *WHP SAC Technical Report No.2*, WOCE Report No. 143/96 [unpublished manuscript].

Gouretski, V.V. and K. Jancke (1998) A new World Ocean Climatology: objective analysis on neutral surfaces. *WHP Special Analysis Centre, Technical Report No. 3*. [unpublished manuscript]

Gouretski, V.V. and K. Jancke (1999) A Description and Quality Assessment of the Historical Hydrographic Data for the South Pacific Ocean. *Journal of Atmospheric and Ocean Technology*, 16, No. 11, 1791-1815.

Gouretski, V.V. and K. Jancke (2001) Systematic errors as the cause for an apparent deep water property variability: global analysis of the WOCE and historical hydrographic data. *Progress in Oceanography,* Vol. 48(4), p. 337-402.

Holley, S.E. (1998) Assessing nutrient data quality to examine nutrient ratios in the Atlantic Ocean. University of Southampton, Department of Oceanography, MP Thesis, 186pp.

Jackett, D.R. and T. J. McDougall (1995) Minimal adjustment of hydrographic profiles to archieve static stability. *Journal of Atmospheric and Oceanic Technology*, vol. 12, pp. 381-389.

Kuragano, T. and. M. Kamachi (2000) Global statistical space-time scales of oceanic variability estimated from the TOPEX/POSEIDON altimeter data. *Journal of Geophysical Research*, vol. 105, p. 955-974.

Levitus, S. (1982) Climatological Atlas of the World Ocean, U.S.Gov. Printing Office, Washington, D.C., 173pp.

Levitus, S. , R. Bargett and T. Boyer (1994a) World Ocean Atlas 1994. Vol.3: Salinity. NOAA Atlas NESDID 3, U.S.Gov. Printing Office, Washington D.C., 99 pp.

Levitus, S. and T. Boyer (1994a) World Ocean Atlas 1994. Vol.2: Oxygen. NOAA Atlas NESDID 2, U.S.Gov. Printing Office, Washington D.C., 186 pp.

Levitus, S. and T. Boyer (1994b) World Ocean Atlas 1994. Vol.4: Temperature. NOAA Atlas NESDID 2, U.S.Gov. Printing Office, Washington D.C., 117 pp.

Levitus, S., T.P. Boyer, M.E. Conkright, T. O'Brian, J. Antonov, C. Stephens, L. Stathopolos, D. Johnson and R. Gelfeld (1998). World Ocean Database 1998. Vol. 1: Introduction. NOAA Atlas NESDID 18, U.S.Gov. Printing Office, Washington, D.C., 346 pp.

Lozier, M.S., M.S. McCartney, and W.B. Owens (1994) Anomalous anomalies in averaged hydrographic data. *J. Phys. Oceanography*, 24(12), p. 2624-2638.

Lozier, M.S, Owens, W.B., Curry, R.G. (1995). The climatology of the North Atlantic*. Progress in Oceanography*, 36, 1-44.

McIntosh, P.C. (1990) Oceanographic data interpolation: Objective analysis and splines. *Journal of Geophysical Research*, 95, 13,529-13,541.

Meyers, G., H. Phillips, N. Smith and J. Sprintall (1991) Space and time scales for optimal interpolation of temperature Tropical Pacific Ocean. *Progress in Oceanography*, Vol. 28, pp.189-218.

Olbers, D., V.V. Gouretski, G. Seiß and J. Schröter (1992) Hydrographic atlas of the Southern Ocean. Bremerhaven: Alfred-Wegener-Institute, 17 pp., 82 plates.

Siedler, G. (1998) SI Units in Oceanography, Berichte des Institut für Meereskunde, Kiel, No. 101, 3rd revised edition, 18 pp.1998

Sokolov, S. and S.R. Rintoul (1999) Some remarks on interpolation of nonstationary oceanographic fields. *Journal of Atmospheric and Oceanic Technology*, 16, 1434-1449.

Sterl, A. (2001) On the impact of gap-filling algorithms on variability patterns of reconstracted oceanic surface fields. *Geophysical Research Letters*, 28, N12, p.2473-2476.

WOCE Operations Manual (1991) Requirements for WOCE hydrographic programme data reporting. WHPO Publication 90-1 Revision 1, *WOCE Report 67/91*, Woods Hole, USA,71 pp. (UNPUBLISHED MANUSCRIPT).

Worthington, L.V. (1976). On the North Atlantic Circulation. *The John Hopkins Oceanographic Studies*, 6, 110 pp.
Worthington, L.V., W.R. Wright (1970). North Atlantic Ocean Atlas of potential temperature and salinity in the deep water including temperature, salinity and oxygen profiles from Erica Dan cruise of 1962*. Woods Hole Oceanographic Institution Atlas Series,* 2, 24 pp., 58 plates.

Wunsch, C. (1996). *The Ocean Circulation Inverse Problem. Cambridge*, Cambridge University Press, 442 pp.

Appendix

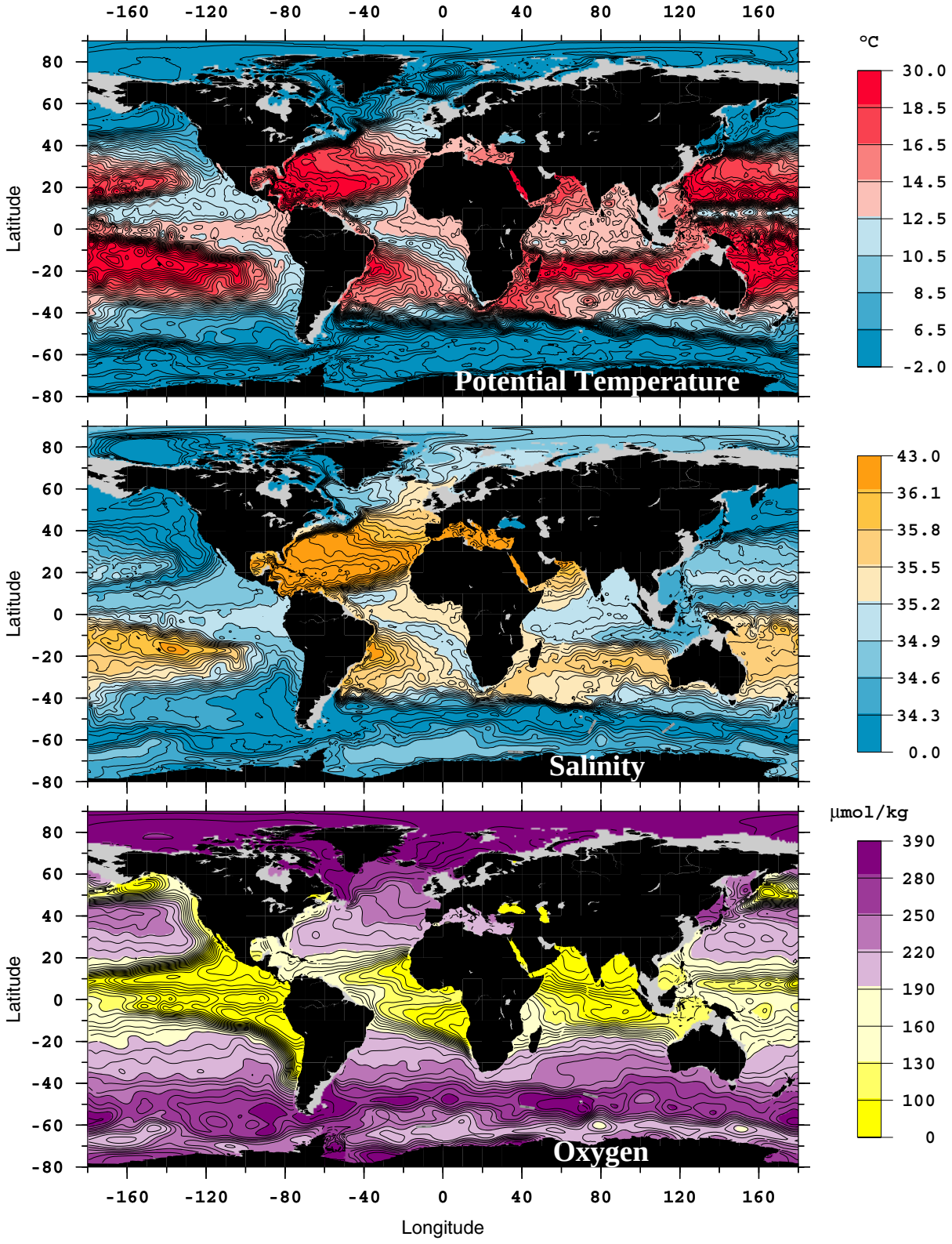
-160
-120
-80
-40
0
40
80
120
160
Latitude
Longitude
Potential Temperature
°C
30.0
18.5
16.5
14.5
12.5
10.5
8.5
6.5
-2.0
Salinity
43.0
36.1
35.8
35.5
35.2
34.9
34.6
34.3
0.0
Oxygen
µmol/kg
390
280
250
220
190
160
130
100
0

Fig. A1a: Annual mean potential temperature, salinity and oxygen at 200 m depth.

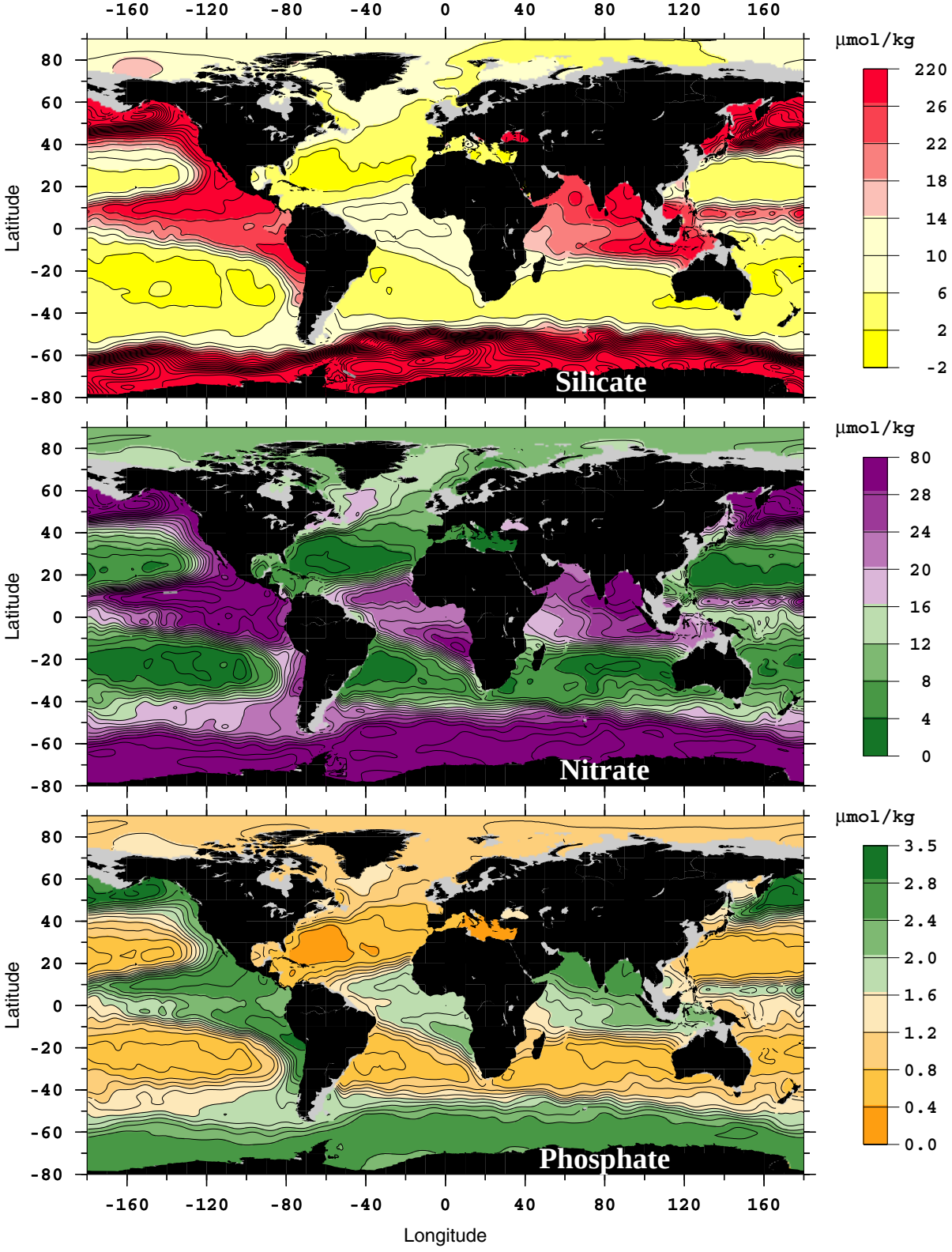

Fig. A1b: Annual mean silicate, nitrate and phosphate at 200 m depth.

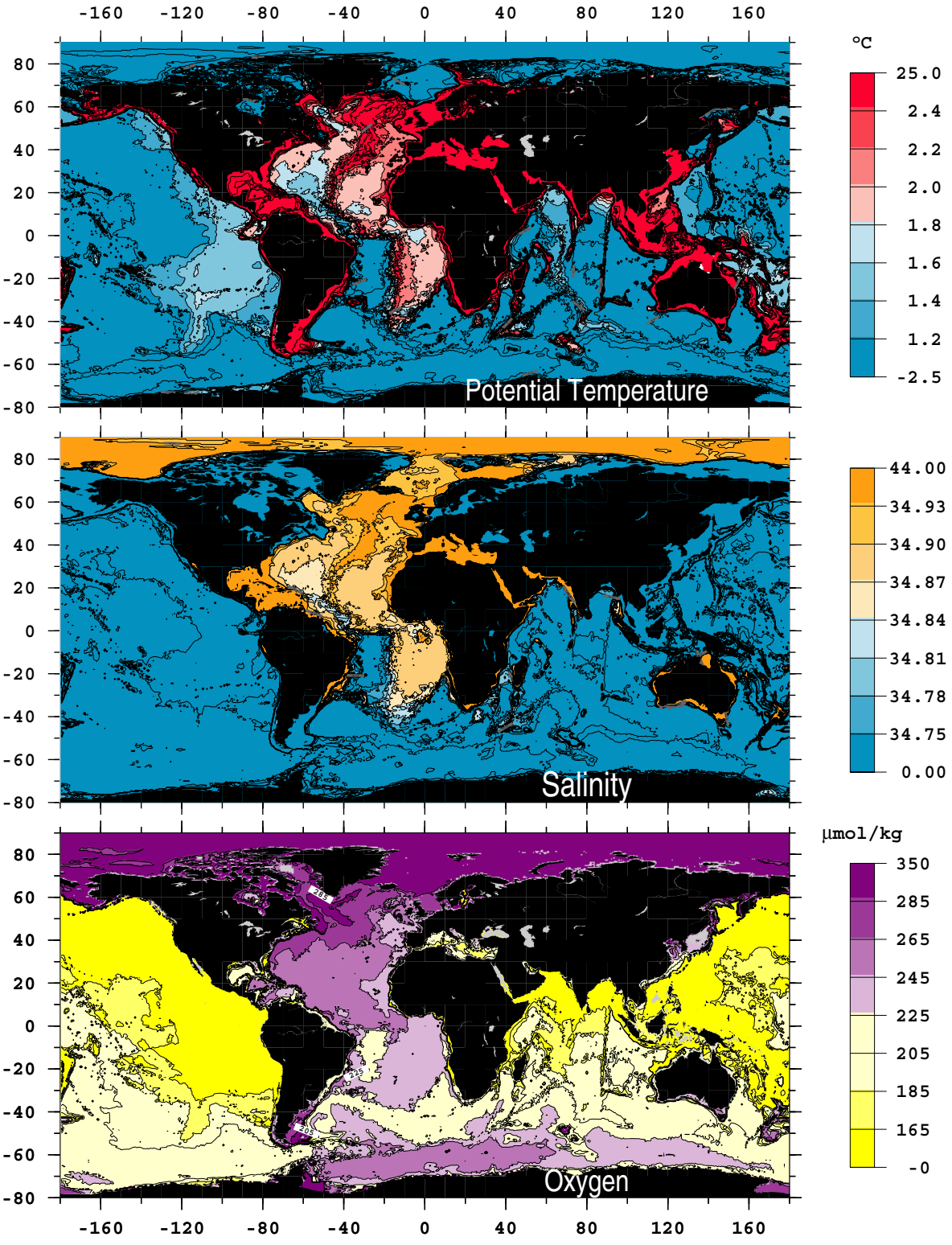

Fig. A1c: Annual mean near-bottom potential temperature, salinity, and oxygen.

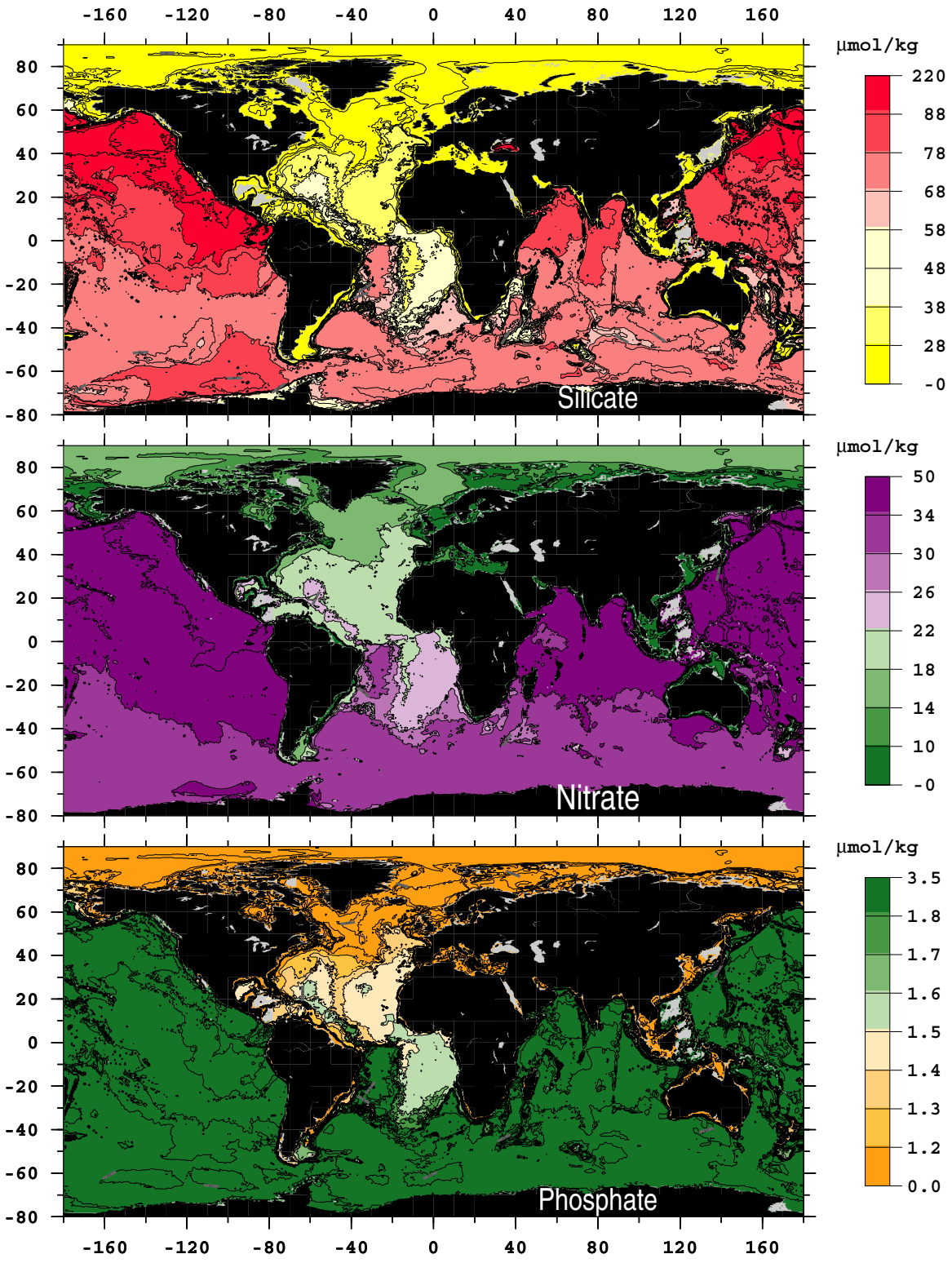

Fig. A1d: Annual mean near-bottom silicate, nitrate and phosphate.

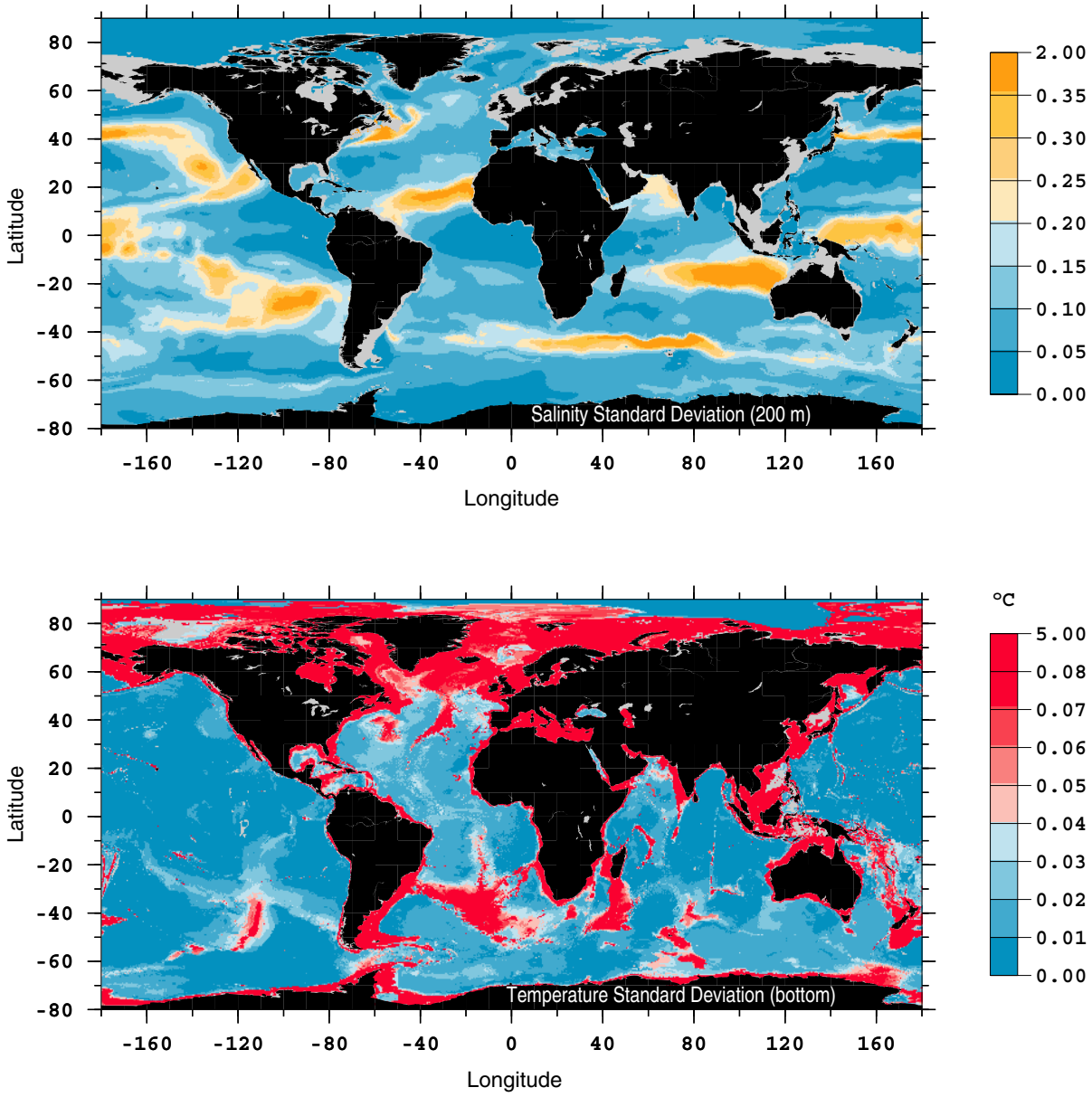

Fig. A2: Standard deviations for salinity at 200 meter level and for near-bottom potential temperature. (Standard deviations are computed on isopycnal surfaces within the influence bubble)

Autoren/Authors

Viktor V. Gouretski * +49-40-42838-7621 gouretsk@ifm.uni-hamburg.de

Klaus Peter Koltermann +49-40-3190-3500 koltermann@bsh.de

Bundesamt für Seeschifffahrt und Hydrographie
Bernhard-Nocht-Strasse 78 Postfach 30 12 20
D-20359 Hamburg 20305 Hamburg
Germany

* Institut für Meereskunde
Universität Hamburg
Zentrum für Meeres- und Klimaforschung
Bundesstr. 53
D-20146 Hamburg
Germany

Berichte des Bundesamtes für Seeschiffahrt und Hydrographie

Verzeichnis der veröffentlichten Arbeiten

1	(1994)	Sy, A., Ulrich, J.	North Atlantic Ship-of-Opportunity XBT Programme 1990 - Data Report, 134 pp.
2	(1994)	Hagen, E., Mittelstaedt, E., Feistel, R., Klein, H.	Hydrographische Untersuchungen im Ostrandstromsystem vor Portugal und Marokko 1991 - 1992, 49 pp.
3	(1994)	Oliczewski, J., Schmidt, D.	Entwicklung einer Bestrahlungsapparatur zum photochemischen Aufschluß von Meerwasserproben zur Bestimmung von Schwermetallen, 70 pp.
4	(1994)	BSH [Hrsg.]	Das UN-Seerechtsübereinkommen tritt in Kraft: Inhalte und Konsequenzen für die Bundesrepublik Deutschland, 71 pp.
5	(1995)	BSH [Hrsg.]	Nationale Folgerungen aus dem Inkrafttreten des UN-Seerechtsübereinkommens, 103 pp.
6	(1995)	Haffer, E., Schmidt, D.	Entwicklung eines Probenvorbereitungsverfahrens zur Bestimmung von Arsen im Meerwasser mit der Totalreflexions-Röntgenfluoreszenzanalyse, 109 pp.
7	(1995)	BSH [Hrsg.]	Global Ocean Observing System - Statusbericht, 100 pp.
8	(1996)	Mittelstaedt, E., Meincke, J., Klein, H.	WOCE-Current measurements: The ACM8 array – Data Report, 150 pp.
9	(1996)	BSH [Hrsg]	GOOS Workshop - Anforderungen an ein wissenschaftliches Konzept für den deutschen Beitrag, 60 pp.
10	(1997)	Sterzenbach, D.	Entwicklung eines Analyseverfahrens zur Bestimmung von chlorierten Kohlenwasserstoffen in marinen Sedimenten und Schwebstoffen unter besonderer Berücksichtigung der überkritischen Fluidextraktion, 233 pp.
11	(1997)	Jonas, M., Richter, R.	Stand und Entwicklungstendenzen nautischer Systeme, Anlagen und Geräte an Bord von Seeschiffen, 37 pp.
12	(1997)	Wedekind, C., Gabriel, H., Goroncy, I., Främke, G., Kautsky, H.	"Meteor"-Reise Nr. 71/1985, Norwegen-Grönlandsee – Datenbericht. 44 pp.
13	(1998)	BSH [Hrsg]	HELCOM Scientific Workshop - The Effects of the 1997 Flood of the Odra and Vistula Rivers. 46 pp.
14	(1998)	Berger, R., Klein, H., Mittelstaedt, E., Ricklefs, K., Ross, J.	Der Wasseraustausch im Tidebecken Hörnum-Tief – Datenreport. 260 pp.
15	(1998)	Röske, F.	Wasserstandsvorhersage mittels neuronaler Netze. 212 pp.
16	(1998)	Ross, J., Mittelstaedt, E. Klein, H., Berger, R., Ricklefs, K.	Der Wasseraustausch im Tidebecken Hörnum-Tief – Abschlußbericht. 98 pp.
17	(1998)	Klein, H.	OPUS-Current Measurements: Mecklenburg Bight and Fehmarnbelt - Data Report, 150 pp.
18	(1999)	BSH [Hrsg]	Deutscher Programmbeitrag zum Globalen Ozeanbeobachtungssystem (GOOS), 67 pp.
19 pp.	(1999)	BSH [Hrsg]	German Programme Contribution to the Global Ocean Observing System (GOOS), 71
20	(1999)	Sztobryn, M., Stanislawczyk, I., Schmelzer, N.	Ice Conditions in the Szczecin and Pomeranian Bay During the Normal Period from 1961-1990, 36 pp.

21	(1999)	Nies, H., Karcher, M., Bahe, C., Backhaus, J., Harms, I.	Transportmechanismen radioaktiver Substanzen im Arktischen Ozean - Numerische und experimentelle Studien am Beispiel der Barents- und Karasee, 134 pp.
22	(2000)	Lorbacher, K.	Niederfrequente Variabilität meridionaler Transporte in der Divergenzzone des nordatlantischen Subtropen- und Subpolarwirbels – Der WOCE-Schnitt A2, 156 pp.
23	(2000)	Klein, H.	The Subsurface Eastern Boundary Current of the North Atlantic between 32°N and 53°N – Data Report, 240 pp.
24	(2000)	Klein, H.	Strömungen und Seegangsverhältnisse westlich der Insel Hiddensee - Datenreport, 59 pp.
25	(2001)	Goedecke, E.	Der hydrographische Aufbau in der Deutschen Bucht vornehmlich dargestellt auf Grund der vorliegenden Unterlagen über Temperatur, Salzgehalt und Dichte, 202 pp.
26	(2001)	Klein, H., Mittelstaedt, E.	Strömungen und Seegangsverhältnisse vor Graal-Müritz und in der Tromper Wiek - Datenreport, 162 pp.
27	(2001)	Klein, H., Mittelstaedt, E.	Gezeitenströme und Tidekurven im Nahfeld von Helgoland, 24 pp. und Anhang.
28	(2001)	Behnke, J., Berking, B., Herberg, J., Jonas, M., Mathes, S.	Functional Scope and Model of Integrated Navigation Systems - A Toolbox for Identification and Testing. 181 pp.
29	(2001)	Dick, S., Kleine, E., Müller-Navarra, S., Klein, H., Komo, H.	The Operational Circulation Model of BSH (BSHcmod) – Model description and validation. 49 pp.
30	(2002)	Sy, A. , Ulrich, J., Weichert, H.-J.	Upper Ocean Climate Ship-of-Opportunity Programme of BSH – A Status Report. 45 pp.
31	(2003)	Dahlmann, G.	Characteristic Features of Different Oil Types in Oil Spill Identification. 48 pp.
32	(2003)	Nies, H., Gaul, H., Oestereich, F., Albrecht, H., Schmolke, S., Theobald, N., Becker, G., Schulz, A., Frohse, A., Dick, S., Müller-Navarra, S., Herklotz, K.	Die Auswirkungen des Elbehochwassers vom August 2002 auf die Deutsche Bucht. 81 pp.
33	(2003)	Loewe, P., Becker, G., Brockmann, U., Frohse, A., Herklotz, K., Klein, H., Schulz, A.	Nordsee und Deutsche Bucht 2002 – Ozeanographischer Zustandsbericht
34	(2004)	Schulz, G.	Geomagnetic Results Wingst 1996, 1997, 1998 and 1999 including the complete Wingst date set since 1939 on CDrom
35	(2004)	Gouretski, V. V., Koltermann, K.P.	WOCE Global Hydrographic Climatology
36	(2004)	Gayer, G., Dick, S., Pleskachevsky, A., Rosenthal, W.	Modellierung von Schwebstofftransporten in Nord- und Ostsee